

Chapter 11

Tectonic and Structural Evolution of the Anadarko Basin and Structural Interpretation and Modeling of a Composite Regional 2D Seismic Line



Click here to return to
Volume Title Page

By Ofori N. Pearson and John J. Miller

Chapter 11 of 13

Petroleum Systems and Assessment of Undiscovered Oil and Gas in the Anadarko Basin Province, Colorado, Kansas, Oklahoma, and Texas—USGS Province 58

Compiled by Debra K. Higley

U.S. Geological Survey Digital Data Series DDS-69-EE

U.S. Department of the Interior
SALLY JEWELL, Secretary

U.S. Geological Survey
Suzette M. Kimball, Acting Director

U.S. Geological Survey, Reston, Virginia: 2014

For more information on the USGS—the Federal source for science about the Earth, its natural and living resources, natural hazards, and the environment, visit <http://www.usgs.gov> or call 1–888–ASK–USGS.

For an overview of USGS information products, including maps, imagery, and publications, visit <http://www.usgs.gov/pubprod>

To order this and other USGS information products, visit <http://store.usgs.gov>

Any use of trade, firm, or product names is for descriptive purposes only and does not imply endorsement by the U.S. Government.

Although this information product, for the most part, is in the public domain, it also may contain copyrighted materials as noted in the text. Permission to reproduce copyrighted items must be secured from the copyright owner.

Suggested citation:

Pearson, O.N., and Miller, J.J., 2014, Tectonic and structural evolution of the Anadarko Basin and structural interpretation and modeling of a composite regional two-dimensional seismic line, chap. 11, *in* Higley, D.K., compiler, Petroleum systems and assessment of undiscovered oil and gas in the Anadarko Basin Province, Colorado, Kansas, Oklahoma, and Texas—USGS Province 58: U.S. Geological Survey Digital Data Series DDS–69–EE, 23 p., <http://dx.doi.org/10.3133/ds69EE>.

ISSN 2327-638X (online)

Contents

Abstract.....	1
Introduction.....	1
Tectonic, Structural, and Stratigraphic Overview.....	1
Precambrian Crustal Consolidation.....	3
Late Precambrian to Middle Cambrian Development of the Southern Oklahoma Aulacogen.....	6
Late Cambrian to Early Mississippian Isostatic Subsidence	7
Late Mississippian to Early Permian Development of the Anadarko Basin.....	8
Stratigraphic Overview	9
Cambrian and Ordovician Rocks.....	9
Silurian, Devonian, and Mississippian Rocks	9
Pennsylvanian Rocks	10
Permian Rocks.....	10
2D Reflection Seismic Datasets Available to the U.S. Geological Survey	11
2D Reflection Seismic Data Interpretation.....	13
General Description of the Seismic Lines	13
Seismic Interpretation of the Anadarko Composite Seismic Line.....	16
Structural Restoration of the Anadarko Composite Seismic Line	17
Summary.....	21
Acknowledgments.....	21
References Cited.....	21

Figures

1. Map showing the location of the Anadarko Basin Province (red line). The general outline of the Anadarko Basin (blue line) is from Johnson and others (1988).....2
2. Map showing the location of seismic lines (blue) licensed by the USGS within the Anadarko Basin Province (red line). Names by which the seismic lines are referred are also shown. Seismic data are owned or controlled by Seismic Exchange, Inc2
3. Map showing the major structural provinces of the Anadarko Basin and adjacent areas. Traces of major thrust faults are also shown in red, with U and D designating the upthrown and downthrown sides of selected faults. The fault system on the northern edge of the Wichita and Amarillo uplifts is known as the Wichita fault system (Harlton, 1963). Faults specifically referred to in the text are labeled. State boundaries are outlined in black; counties are outlined in gray. Modified from Luza and others (1987), Johnson (1989), and Luza (1989). Traces of seismic lines are shown in light blue.....3
4. Simplified stratigraphic column for the northern Anadarko Basin (modified from Higley and Gaswirth, 2014, and references therein). Informal unit names are italicized. Names in red are the stratigraphic units used in the seismic interpretation and structural restoration. Wavy horizontal lines and vertical bars indicate unconformities. Ages are in millions of years before the present (Ma). Note the change of vertical scale between the Cambrian–Mississippian column and the Pennsylvanian–Permian column

5. Maps showing the sequence of Proterozoic events that formed the complex suite of basement rocks beneath the Anadarko Basin Province. Modified from Whitmeyer and Karlstrom (2007). *A*, Yavapai orogeny; *B*, intrusion of the Yavapai Province by granitoids; *C*, Mazatzal orogeny; *D*, intrusion of Mazatzal granitoids; *E*, suturing of the Granite-Rhyolite Province; *F*, extensive granitoid intrusion of the Yavapai, Mazatzal, and Granite-Rhyolite Provinces; *G*, intrusion of Grenville-aged granitoids and development of the Midcontinent rift system; *H*, development of the southern Oklahoma aulacogen. Ga, billion years before the present5
6. Map showing the geometry of the eastern Laurentian margin during the Cambrian in the southern and eastern United States. Locations and geometries of the southern Oklahoma aulacogen and the Reelfoot rift are shown. Paleogeographic map for the Middle Cambrian (510 Ma) is from Blakey (2011). Rifted margin geometry and location of the Reelfoot rift and southern Oklahoma aulacogen are from Keller and others (1983).....6
7. Map showing the location of the northwestern limits of the southern Oklahoma aulacogen relative to the present Anadarko Basin. The aulacogen is shown in light gray, thrust and reverse faults of the Wichita fault system are shown in red, and contour lines show approximate depths to basement in the Anadarko Basin, with depths in tens of thousands of feet below sea level. Modified from Perry (1989) and references therein. Ga, billions of years before the present7
8. Root mean square velocity model used to migrate and convert seismic Line D. Velocities were determined using an automated velocity picking algorithm, and subsequently smoothed using a 201 common depth point horizontal, and 250-millisecond vertical, smoothing operator. A color bar illustrating the velocity scale is also shown. Seismic data are owned or controlled by Seismic Exchange, Inc.; interpretation is that of the U.S. Geological Survey.....12
9. Uninterpreted seismic Line A. Location of line is shown in figure 2. Horizontal and vertical scales are equal. Black colors are amplitude peaks; red colors are amplitude troughs. Seismic data are owned or controlled by Seismic Exchange, Inc13
10. Uninterpreted seismic Line B. Location of line is shown in figure 2. Horizontal and vertical scales are equal. Dark black colors are amplitude peaks; dark red colors are amplitude troughs. Seismic data are owned or controlled by Seismic Exchange, Inc. Figure 10 is oversized. Click on the thumbnail to view the enlarged version14
11. Uninterpreted seismic Line C. Location of line is shown in figure 2. Horizontal and vertical scales are equal. Dark black colors are amplitude peaks; dark red colors are amplitude troughs. Seismic data are owned or controlled by Seismic Exchange, Inc14
12. Uninterpreted seismic Line D. Location of line is shown in figure 2. Horizontal and vertical scales are equal. Dark black colors are amplitude peaks; dark red colors are amplitude troughs. Seismic data are owned or controlled by Seismic Exchange, Inc. Figure 12 is oversized. Click on the thumbnail to view the enlarged version15
13. Uninterpreted seismic Line E. Location of line is shown in figure 2. Horizontal and vertical scales are equal. Dark black colors are amplitude peaks; dark red colors are amplitude troughs. Seismic data are owned or controlled by Seismic Exchange, Inc. Figure 13 is oversized. Click on the thumbnail to view the enlarged version15

14. Map showing the location of wells used to aid in the interpretation of the composite seismic line. Oklahoma counties are shown in gray. The segments of the composite seismic line are shown in blue. American Petroleum Institute well numbers are given.....	16
15. Interpreted seismic Line C. Location of line is shown in figure 2. Horizontal and vertical scales are equal. Dark black colors are amplitude peaks; dark red colors are amplitude troughs. Well symbols are the same as those used in fig. 14. American Petroleum Institute well numbers are indicated. Lithology codes for well tops are given in table 1. Seismic data are owned or controlled by Seismic Exchange, Inc.; interpretation is that of the U.S. Geological Survey	17
16. Interpreted seismic Line D. Location of line is shown in figure 2. Horizontal and vertical scales are equal. Dark black colors are amplitude peaks; dark red colors are amplitude troughs. Well symbols are the same as those used in fig. 14. American Petroleum Institute well numbers are indicated. Lithology codes for well tops are given in table 1. Seismic data are owned or controlled by Seismic Exchange, Inc.; interpretation is that of the U.S. Geological Survey. Figure 16 is oversized. Click on the thumbnail to view the enlarged version	18
17. Interpreted seismic Line E. Location of line is shown in figure 2. Horizontal and vertical scales are equal. Dark black colors are amplitude peaks; dark red colors are amplitude troughs. Well symbols are the same as those used in figure 14. American Petroleum Institute well numbers are indicated. Lithology codes for well tops are given in table 1. Seismic data are owned or controlled by Seismic Exchange, Inc.; interpretation is that of the U.S. Geological Survey. Figure 17 is oversized. Click on the thumbnail to view the enlarged version	18
18. Structural restoration showing individual restoration stages. Depth in each stage is shown in thousands of feet below sea level; horizontal distance is given in miles from the southwestern edge of seismic Line C (no vertical exaggeration). Seismic data are owned or controlled by Seismic Exchange, Inc.; interpretation is that of the U.S. Geological Survey. Figure 18 is oversized. Click on the thumbnail to view the enlarged version	18
19. Incremental shortening (blue line and round markers) and cumulative shortening (red line and star markers) is shown for all stages of the structural restoration shown in figure 18. Note that the vertical axis is time, rather than stratigraphic thickness	20

Tables

1. Lithology codes and corresponding stratigraphic units for formation tops shown in figures 15, 16, and 17	10
2. Seismic line names, counties and states where seismic lines were recorded, the year the USGS purchased licenses for the data, and the lengths of each line. Seismic data are owned or controlled by Seismic Exchange, Inc.; interpretation is that of the U.S. Geological Survey	11
3. Data acquisition parameters for the five seismic lines used in this study. Seismic data are owned or controlled by Seismic Exchange, Inc.; interpretation is that of the U.S. Geological Survey.....	11

Tectonic and Structural Evolution of the Anadarko Basin and Structural Interpretation and Modeling of a Composite Regional 2D Seismic Line

By Ofori N. Pearson and John J. Miller

Abstract

The U.S. Geological Survey recently completed an assessment of undiscovered oil and gas resources in the Anadarko Basin Province of western Oklahoma and Kansas, northern Texas, and southeastern Colorado. The assessment methodology required a detailed look at the region's tectonic and structural evolution, which can be divided into the following four periods: (1) Precambrian crustal consolidation; (2) development of the southern Oklahoma aulacogen during late Precambrian to Middle Cambrian time; (3) thermally controlled isostatic subsidence of the failed rift from Late Cambrian to Early Mississippian time; and (4) development of the Ouachita-Marathon orogeny that caused the Wichita uplift and development of the asymmetric Anadarko Basin beginning in Late Mississippian time. Many of the basin's key structural elements are visible on two-dimensional reflection seismic lines, and interpretations of the data reveal the basin's subsurface structural geometry. A structural restoration based upon the seismic interpretation shows the possible geometric evolution for 22 of the Anadarko Basin's key stratigraphic units.

Introduction

The asymmetric Anadarko Basin (fig. 1) is the deepest interior cratonic basin in the conterminous United States, containing as much as $\approx 40,000$ feet of Upper Cambrian–Permian sedimentary rocks (Johnson and others, 1988). It has been one of the more productive U.S. basins in terms of production of oil and gas, with cumulative production in excess of 5.4 billion barrels of oil and 125 trillion cubic feet of gas (IHS Energy, 2010). In 2010, the U.S. Geological Survey (USGS) conducted an assessment of undiscovered oil and gas resources contained within the Anadarko Basin Province of western Oklahoma and Kansas, northern Texas, and southeastern Colorado (fig. 1), resulting in means of 495 million barrels of oil, 27,461 billion cubic feet of gas, and 410 million barrels of natural gas liquids (Higley and others, 2011).

As part of the 2010 assessment, an analysis of the Anadarko Basin's tectonic and structural evolution was conducted. A broad overview is presented in this chapter of the report, based on previously published studies and an interpretation and structural restoration of five two-dimensional (2D) reflection seismic lines (fig. 2) acquired by the USGS within the basin. Published studies typically describe four main phases of tectonic and structural activity for the Anadarko Basin, and those divisions are adopted for this study. The acquisition and processing of the reflection seismic lines are also described. Three of those lines (fig. 2; Lines C, D, and E) that lie in close proximity to one another were combined into a composite regional line, and the seismic interpretation of this line is discussed. A structural restoration is documented that was built from the seismic interpretation and key findings of the restoration are tied into elements of the broader tectonic and structural evolution of the Anadarko Basin.

Tectonic, Structural, and Stratigraphic Overview

Although the oldest sedimentary rocks in the Anadarko Basin are of Cambrian age, the basin's earlier tectonic and structural history plays an important role in the depositional history of the Paleozoic section and on the petroleum systems that are the subject of the 2010 USGS assessment. The eastern margin of North America has undergone two complete Wilson cycles (plate-tectonic spreading and convergence; Wilson, 1966)—the assembly and breakup of both the Rodinia and Pangaea land masses. Basement and sedimentary rocks of the Anadarko Basin Province were involved in the Proterozoic assembly and breakup of Rodinia, and the Paleozoic assembly of Pangaea.

Most workers describe the evolution of the Anadarko Basin in terms of four main tectonic and structural events, two of which occurred before deposition of the basin's oldest (Cambrian) sedimentary rocks. These four primary phases of tectonic and structural activity are: (1) Precambrian crustal

2 Tectonic and Structural Evolution of the Anadarko Basin, Structural Interpretation and Modeling of a Seismic Line

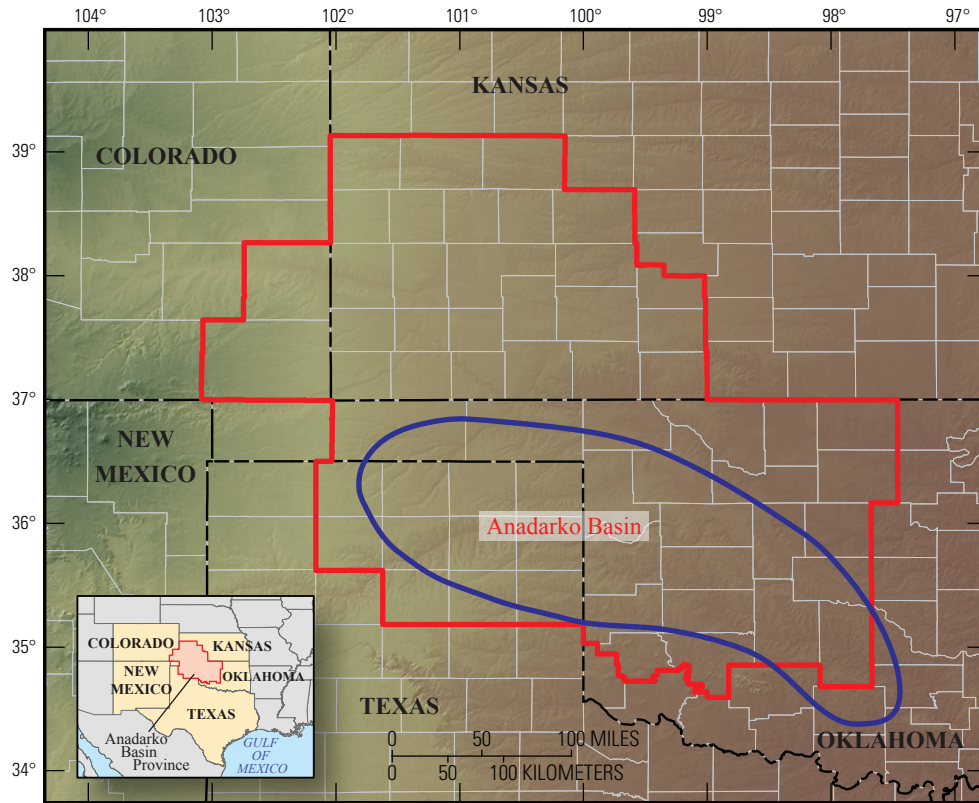


Figure 1. Map showing the location of the Anadarko Basin Province (red line). The general outline of the Anadarko Basin (blue line) is from Johnson and others (1988).

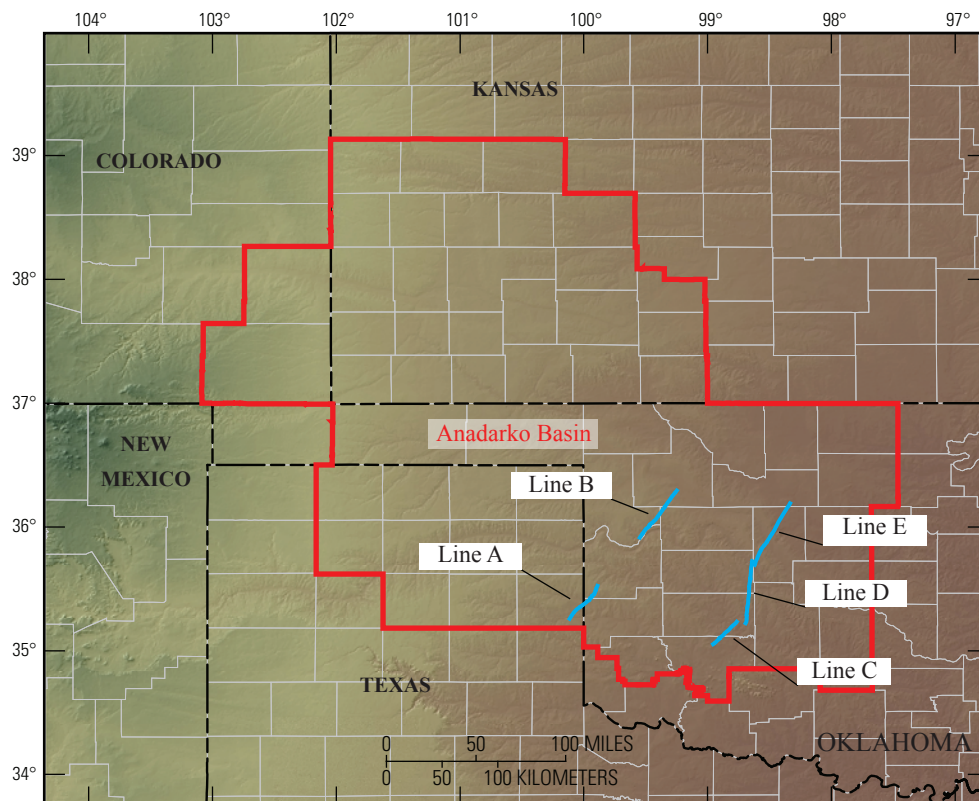


Figure 2. Map showing the location of seismic lines (blue) licensed by the USGS within the Anadarko Basin Province (red line). Names by which the seismic lines are referred are also shown. Seismic data are owned or controlled by Seismic Exchange, Inc.

consolidation; (2) late Precambrian to Middle Cambrian development of the southern Oklahoma aulacogen; (3) Late Cambrian to Early Mississippian isostatic subsidence; and (4) development of the Anadarko Basin beginning in the Late Mississippian, because of the Ouachita orogeny. The following discussion gives a broad overview of each of these four phases, primarily as they relate to the Anadarko Basin proper. Although the Anadarko Basin Province also contains parts of other major structural elements (fig. 3) that make up the southern midcontinent region (for example, the Hugoton embayment, the Cimarron arch, the Palo Duro Basin, and the Nemaha uplift), these are discussed only in terms of how they relate to the Anadarko Basin. A simplified stratigraphic column for the basin is shown in figure 4. A rationale for the simplification shown in the column and a description of the lithologies are provided in the stratigraphic summary portion of this report.

Precambrian Crustal Consolidation

Figure 5 (modified from Whitmeyer and Karlstrom, 2007) portrays the Proterozoic sequence of events that led to crustal consolidation of basement rock beneath the Anadarko Basin Province. Also shown in figure 5 are the ages of rocks

that were sutured onto the southeastern margin of Laurentia and also the ages of intrusives that accompanied the various orogenies and stitched terranes together. The oldest basement rocks in the province (fig. 5A) were likely accreted onto the margin of Laurentia during the Yavapai orogeny ≈ 1.76 – 1.72 billion years before the present (Ga) (Whitmeyer and Karlstrom, 2007). During the orogeny, oceanic arc terranes (1.76–1.72 Ga) sutured onto Laurentia along the Cheyenne belt in Wyoming and the Spirit Lake tectonic zone at the southern margin of the western Superior and Penokean Provinces (Whitmeyer and Karlstrom, 2007). Following accretion, the Yavapai Province was intruded by granitoids (fig. 5B) dated at ≈ 1.72 – 1.68 Ga (Whitmeyer and Karlstrom, 2007). The next major event to affect the southeastern margin of Laurentia was the Mazatzal orogeny, during which crust dated at 1.69–1.65 Ga formed in continental margin volcanic arcs and back-arc-related supracrustal successions were accreted along a bivergent suture zone (fig. 5C; Whitmeyer and Karlstrom, 2007). During later stages of the Mazatzal orogeny (1.65–1.60 Ga), both the Yavapai and Mazatzal Provinces were intruded by granitoids (fig. 5D). The southernmost portion of the Anadarko Basin Province may be underlain by basement rocks of the 1.55–1.35 Ga Granite-Rhyolite Province (fig. 5E; Van Schmus and others, 1996). Following

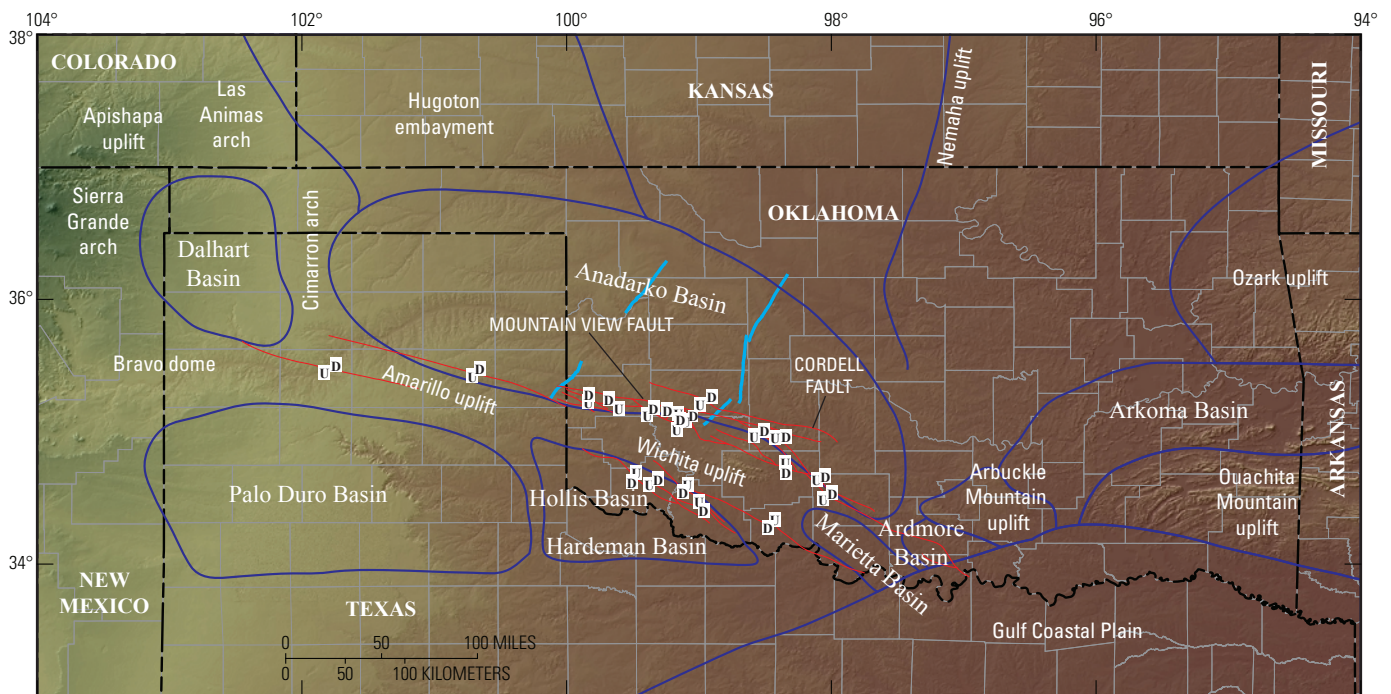


Figure 3. Map showing the major structural provinces of the Anadarko Basin and adjacent areas. Traces of major thrust faults are also shown in red, with U and D designating the upthrown and downthrown sides of selected faults. The fault system on the northern edge of the Wichita and Amarillo uplifts is known as the Wichita fault system (Harlton, 1963). Faults specifically referred to in the text are labeled. State boundaries are outlined in black; counties are outlined in gray. Modified from Luza and others (1987), Johnson (1989), and Luza (1989). Traces of seismic lines are shown in light blue.

4 Tectonic and Structural Evolution of the Anadarko Basin, Structural Interpretation and Modeling of a Seismic Line

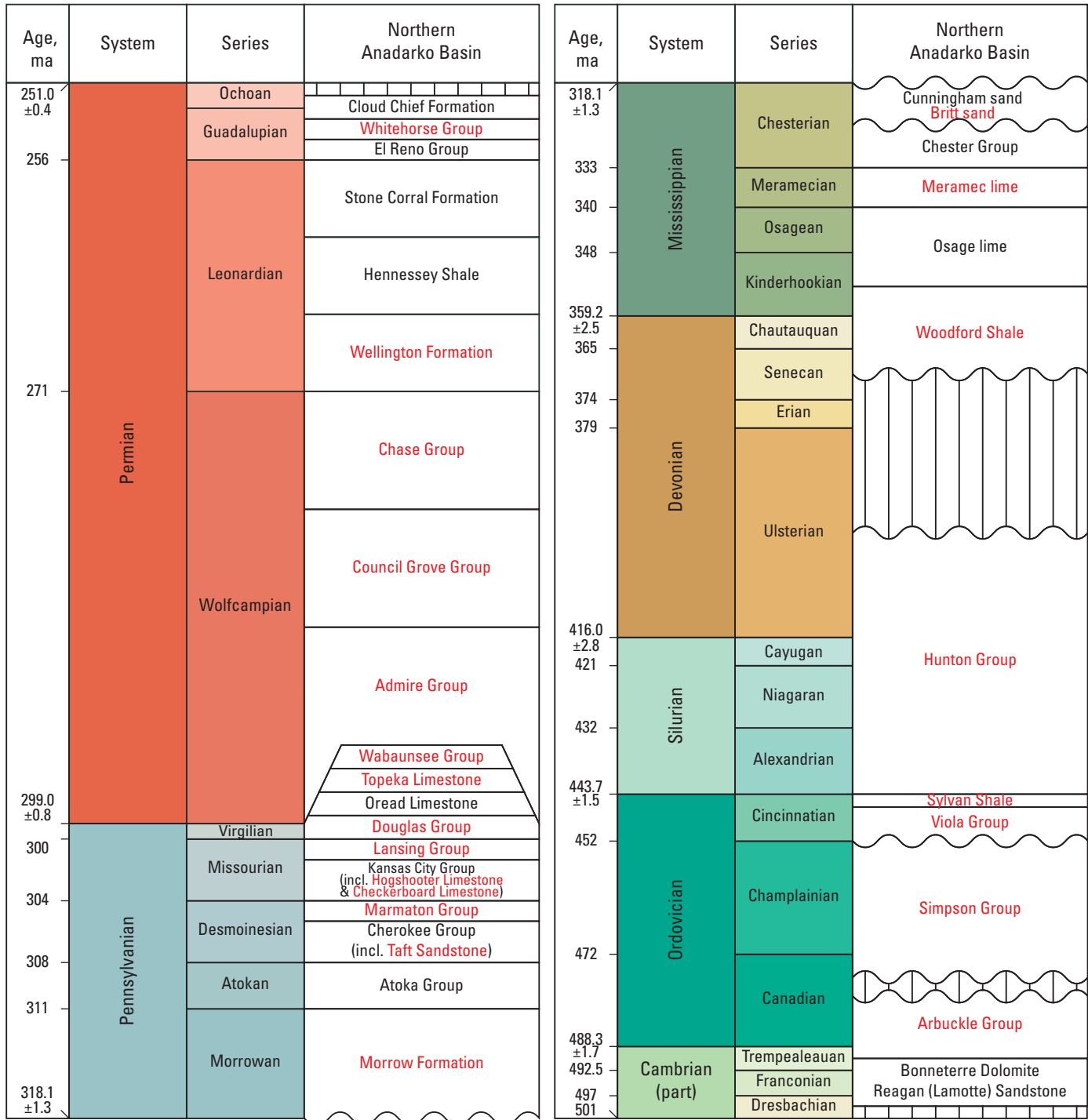


Figure 4. Simplified stratigraphic column for the northern Anadarko Basin (modified from Higley and Gaswirth, 2014, and references therein). Informal unit names are italicized. Names in red are the stratigraphic units used in the seismic interpretation and structural restoration. Wavy horizontal lines and vertical bars indicate unconformities. Ages are in millions of years before the present (Ma). Note the change of vertical scale between the Cambrian–Mississippian column and the Pennsylvanian–Permian column.

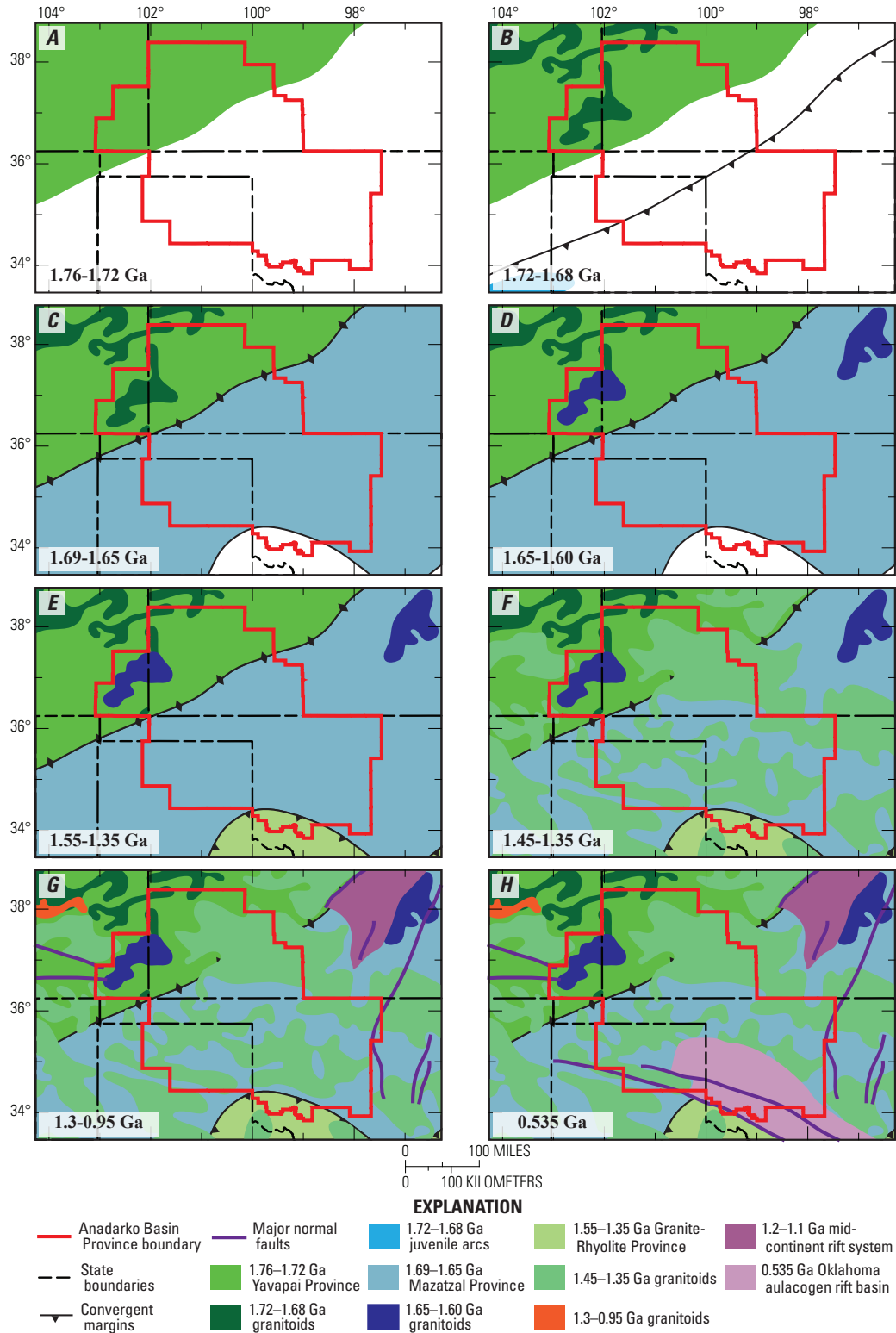


Figure 5. Maps showing the sequence of Proterozoic events that formed the complex suite of basement rocks beneath the Anadarko Basin Province. Modified from Whitmeyer and Karlstrom (2007). *A*, Yavapai orogeny; *B*, intrusion of the Yavapai Province by granitoids; *C*, Mazatzal orogeny; *D*, intrusion of Mazatzal granitoids; *E*, suturing of the Granite-Rhyolite Province; *F*, extensive granitoid intrusion of the Yavapai, Mazatzal, and Granite-Rhyolite Provinces; *G*, intrusion of Grenville-aged granitoids and development of the Midcontinent rift system; *H*, development of the southern Oklahoma aulacogen. Ga, billion years before the present.

accretion of the Granite-Rhyolite Province to the southeastern margin of Laurentia, the Yavapai, Mazatzal, and Granite-Rhyolite Provinces were all intruded by extensive bimodal A-type granites (1.45–1.35 Ga, fig. 5F; Whitmeyer and Karlstrom, 2007) that stitched together the three provinces.

The Proterozoic assembly of Laurentia culminated during the 1.30–0.95 Ga Grenville orogeny (fig. 5G). The Grenville-Llano deformation front (the Llano front is the likely southwestern continuation in Texas of the Grenville front) lay to the south of the Anadarko Basin Province in the Granite-Rhyolite Province (Thomas, 1991), thus probably did not affect basement rocks within the Anadarko Basin Province. Along with the Grenville deformation front, late Grenville granitoid intrusions in Colorado and the southernmost extent of the 1.2–1.1 Ga Midcontinent rift system in Kansas (fig. 5G) are likely the most proximal signatures of the Grenville orogeny. Following the amalgamation of Laurentia during the Grenville orogeny, a long process of diachronous rifting began. Early rifting (between 0.78 and 0.68 Ga) occurred to the west, and separated Australia, Antarctica, south China, and Siberia from Laurentia. Rifting on the eastern margin of Laurentia began between 0.62 and 0.55 Ga (Whitmeyer and Karlstrom, 2007). The final rifting event that affected the midcontinent region was the separation of the Argentinian Precordillera terrane from the Ouachita embayment of eastern Oklahoma and Texas (Thomas and Astini, 1996). Although the mechanics behind the translation of the Argentinian Precordillera from the southeastern margin of Laurentia to the western margin of Gondwana are poorly understood, they likely involve the Reelfoot rift and Southern Oklahoma aulacogen (Whitmeyer and Karlstrom, 2007). Formation of the southern Oklahoma aulacogen (fig. 5H) during the Cambrian (~0.535 Ga) was the next major tectonic and structural event to affect the Anadarko Basin Province.

Late Precambrian to Middle Cambrian Development of the Southern Oklahoma Aulacogen

The second half of the first complete Wilson cycle to affect the eastern margin of North America involved the breakup of Rodinia and the opening of the Iapetus Ocean. Toward the end of this rifting phase in the Early Cambrian, at least two triple junctions developed in what is now the southeastern United States (Whitmeyer and Karlstrom, 2007). Evidence for the presence of these triple junctions includes the Reelfoot rift and the southern Oklahoma aulacogen (fig. 6). Development of the southern Oklahoma aulacogen played a key role in the formation of the Anadarko Basin, as the aulacogen's geometry and thermal effect on the surrounding crust exhibited first-order controls on subsequent depositional and structural trends.

Shatsky (1946) was the first to suggest the presence of an aulacogen in southern Oklahoma. The primary lines of evidence that support the existence of a failed rift system are an

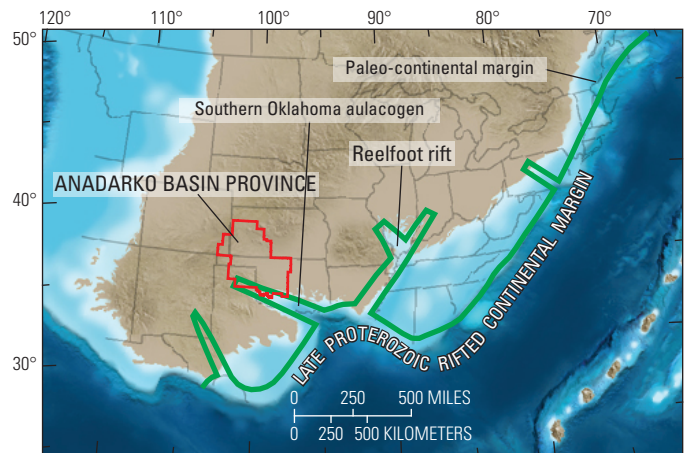


Figure 6. Map showing the geometry of the eastern Laurentian margin during the Cambrian in the southern and eastern United States. Locations and geometries of the southern Oklahoma aulacogen and the Reelfoot rift are shown. Paleogeographic map for the Middle Cambrian (510 Ma) is from Blakey (2011). Rifted margin geometry and location of the Reelfoot rift and southern Oklahoma aulacogen are from Keller and others (1983).

extensive suite of bimodal Cambrian igneous rocks and a linear trend of high Bouguer gravity anomaly values across southern Oklahoma. Bimodal igneous rocks of Cambrian age are well-exposed on the Wichita uplift (fig. 3) south of the Anadarko Basin. These rocks include: (1) the Glen Mountains Layered Complex, which is a layered mafic intrusion; (2) the 525-million years before the present (Ma) Carlton Rhyolite Group, which comprises over 40,000 cubic kilometers (km^3) of silicic intrusive and volcanic rocks (Gilbert, 1983); and (3) other basalts and granites (Keller and Stephenson, 2007). The other primary line of evidence that supports the existence of the southern Oklahoma aulacogen is the linear trend of high Bouguer gravity anomaly values extending from about long. 96° to 101° W. across southern Oklahoma (see fig. 3 of Keller and Stephenson, 2007). This gravity high has been linked to the presence of a deep and massive mafic intrusive (Keller and Baldrige, 1995). The three-armed pattern of Bouguer gravity highs at the southeastern edge of the aulacogen is likely tied to a rift-rift-rift triple junction (see fig. 3 of Keller and Stephenson, 2007).

Rift systems are typically bounded by extensive normal fault systems, and the presence of such faults around the southern Oklahoma aulacogen was inferred by Gilbert (1982, 1987). However, normal fault systems flanking the aulacogen that are clearly rift-related have not been recognized (Keller and Stephenson, 2007). This is likely because of a combination of poor exposures and extensive deformation during the latter parts of the Paleozoic that may have inverted or reactivated Cambrian extensional structures.

Although the axes of the southern Oklahoma aulacogen and the Anadarko Basin are subparallel, the two features do not completely overlap. The northern edge of the aulacogen probably lies beneath the southern edge of the Anadarko Basin

(Perry, 1989; fig. 7). Some of the thrust and reverse faults that separate the basin from the Wichita uplift could be inverted normal faults associated with Cambrian rifting.

By the end of the Middle Cambrian, rifting along the incipient spreading center below southern Oklahoma ended, and the extensive suite of igneous rocks that had been incorporated into the crust in the vicinity of the aulacogen began to cool. This period of thermal subsidence lasted from the Late Cambrian through the Early Mississippian, and characterizes the next major phase in the region's tectonic, structural, and depositional evolution.

Late Cambrian to Early Mississippian Isostatic Subsidence

The oldest sedimentary rocks in the Anadarko Basin are the Upper Cambrian Reagan Sandstone (fig. 4). The deposition of these rocks marks the beginning of a lengthy phase dominated by basin subsidence, during which more than 40,000 ft of Upper Cambrian through Permian sediments

accumulated. The initial phase of subsidence occurred from Late Cambrian through Early Mississippian time, and was dominated by thermally controlled isostatic subsidence caused primarily by cooling of the southern Oklahoma aulacogen (Feinstein, 1981).

This lengthy initial period of subsidence occurred during a time when the southern midcontinent region was isolated from tectonic events related to the start of the second Wilson cycle. In North America, the Appalachian-Ouachita orogenic belt records successive, diachronous orogenies that resulted in the closure of the Iapetus Ocean and the formation of Pangaea during the Permian (Thomas, 2006). These orogenies are the Taconic (Ordovician-Silurian), Acadian (Devonian-Mississippian), and the Alleghanian (Mississippian-Permian). During the Taconic and Acadian orogenies, which mainly affected more northern parts of the North American continent, a passive margin outboard of the southern midcontinent region persisted until Mississippian time (Thomas, 1989). The relative isolation of the southern midcontinent region from tectonic stresses that occurred farther to the north, suggests that unconformities within the Upper Cambrian through Lower

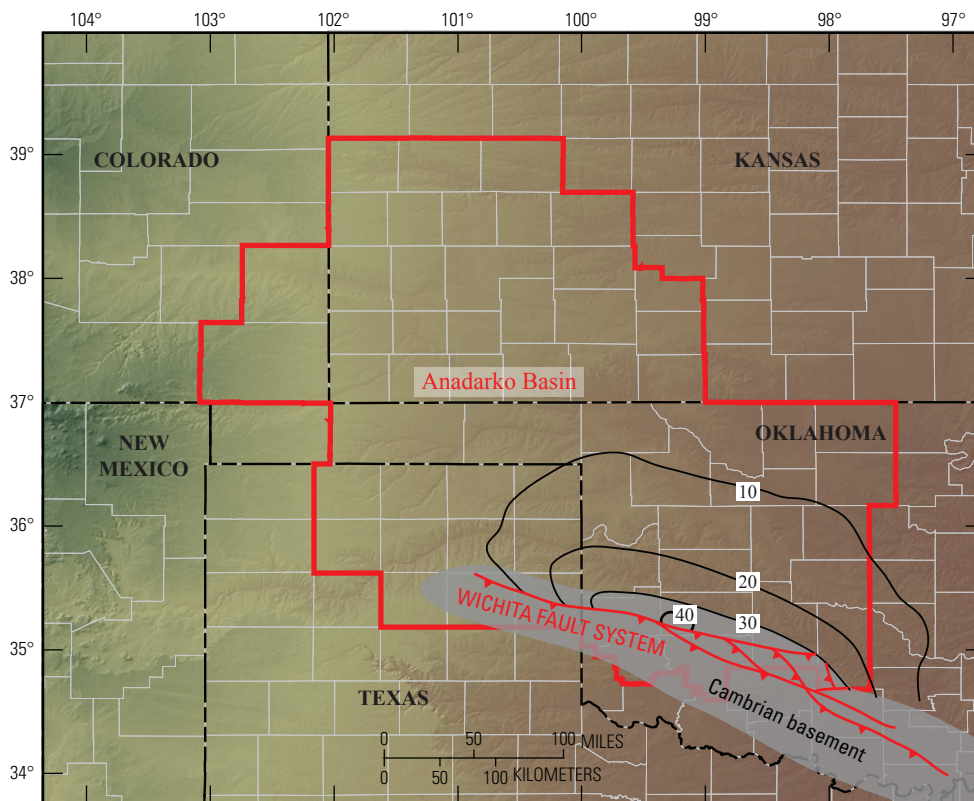


Figure 7. Map showing the location of the northwestern limits of the southern Oklahoma aulacogen relative to the present Anadarko Basin. The aulacogen is shown in light gray, thrust and reverse faults of the Wichita fault system are shown in red, and contour lines show approximate depths to basement in the Anadarko Basin, with depths in tens of thousands of feet below sea level. Modified from Perry (1989) and references therein. Ga, billions of years before the present.

Mississippian stratigraphic section of the Anadarko Basin are more likely related to global sea level changes than to structural events.

The cooling southern Oklahoma aulacogen created accommodation space in what is known as the southern Oklahoma trough, which is generally coincident with the geometry of the aulacogen (Perry, 1989). More than 11,700 ft of Cambrian-Devonian rocks were deposited in this trough (Ham, 1973; Cardott and Lambert, 1985). Feinstein (1981) proposed a two-stage mechanism to explain the Late Cambrian through Early Mississippian subsidence of the Oklahoma trough. The earliest stage occurred during deposition of the basal Upper Cambrian Reagan Sandstone. The rate of subsidence at this stage was low, and can be compared to that of other basins where elastic flexure of the lithosphere in response to an increased load (rocks emplaced during the aulacogen) governed subsidence (Feinstein, 1981). Feinstein (1981) proposed that higher rates of subsidence that followed deposition of the Reagan Sandstone can be attributed to detachment of the aulacogen from the adjacent platform, possibly reactivating normal fault systems that bounded the aulacogen. After detaching from the adjacent platform, evolution of the Oklahoma trough generally followed an exponential curve of subsidence with time controlled by isostatic subsidence driven by cooling of rocks emplaced during formation of the aulacogen (Feinstein, 1981). This two-stage model supports observations that slow initial rates of Cambrian subsidence accelerated during the Early Ordovician before slowing again in the Late Ordovician as the aulacogen reached thermal equilibrium; slow gradual rates of subsidence continued during Silurian, Devonian, and Early Mississippian time (see figs. 2 and 3 in Feinstein, 1981).

Late Mississippian to Early Permian Development of the Anadarko Basin

Beginning in the Late Mississippian, the prolonged period of relative tectonic and structural quiescence in the southern midcontinent region ended abruptly as compressional forces associated with the Appalachian-Ouachita orogeny arrived. For the southern midcontinent region, this marked the onset of the second Wilson cycle, which included the assembly and subsequent breakup of Pangaea. For the remainder of this discussion, this orogenic period will be referred to as the Ouachita-Marathon orogeny, as this nomenclature is more commonly used in the literature to describe the collision between the North American and the South American–African plates. Compressional forces of the Ouachita-Marathon orogeny are generally thought to be responsible for the structural inversion of the southern Oklahoma aulacogen, and the subsequent formation of the Anadarko Basin (Kluth and Coney, 1981; Kluth, 1986).

Structures related to the Ouachita-Marathon orogeny in the Anadarko Basin Province have been extensively documented and described (see, for example, McConnell, 1989; Perry, 1989), as they have not been overprinted by subsequent

deformation. Identification of many of these structures has been aided by the availability of extensive subsurface datasets produced during exploration for petroleum. Detailed descriptions of individual structural features are not provided in the following summary, but the tectonic forces that caused the formation of the Anadarko Basin and the resultant basin-scale structural features are discussed.

The earliest compressional stresses of the Ouachita-Marathon orogeny affected the Alabama promontory during Middle Mississippian time in what is now the Black Warrior Basin of Alabama (Thomas, 2006). The deformation front migrated toward the northwest along the Alabama-Oklahoma transform fault, and reached the Arkoma Basin (fig. 3) by the Early Pennsylvanian (Thomas, 1989). This migration of the deformation front is an excellent example of tectonic inheritance, as preexisting crustal weaknesses that developed during the rifting of Rodinia were exploited by the Ouachita-Marathon orogeny (Thomas, 2006).

Within the Anadarko Basin region, the earliest sign of the approaching deformation front may be the pinching-out of uppermost Mississippian–lowermost Pennsylvanian sandstones in the western Ardmore Basin (fig. 3; Perry, 1989). During Morrowan time, a broad uplift formed that extended from the Criner Hills southward into Texas and northwestward toward the Wichita Mountains. Tomlinson and McBee (1959) called this uplift the Wichita-Criner uplift, and it included the Wichita Mountains, which were rising during this time. To the northeast of the uplift, a narrow trough developed, into which greater thicknesses of Morrowan through Desmoinesian sediments were deposited relative to the shelf farther to the northeast (Johnson, 1989). Development of the Wichita-Criner uplift accelerated during the late Morrowan, and climaxed during Atokan time. On the northeast flank of the Wichita Mountains, synorogenic sediments derived from the weathering of both Mississippian limestones that mantled the Wichita Mountains and basement rocks were deposited in the immediate footwall of the developing Wichita fault system (fig. 3; Johnson, 1989). These synorogenic sediments suggest that the mountains had been unroofed by this time. The Wichita fault system may have reactivated normal faults that formed during emplacement of the southern Oklahoma aulacogen. By the beginning of Desmoinesian time, faulting along the margins of the Wichita Mountains had ended (Perry, 1989). However, the uplift remained a positive feature through the end of the Pennsylvanian, and continued to supply sediments into the deepening Anadarko Basin. During the Late Pennsylvanian, the deformation front appears to have migrated both to the east and to the southwest. The eastward migration is evidenced by structural activity in the Arbuckle Mountains (Perry, 1989) and in the Ouachita Mountains of southeastern Oklahoma and west-central Arkansas (Johnson, 1989). Westward migration is seen by deformation in the Marathon region of western Texas, which climaxed in the Virgilian or Wolfcampian; by Leonardian time, the Ouachita-Marathon orogeny had ended (Kluth and Coney, 1981).

Major structural activity in the Anadarko Basin ended by the Early Permian (Perry, 1989). Deposition continued to the end of the Permian; accommodation space was likely created both by continued gradual subsidence of the basin and compaction of older rocks. The final act of the second Wilson cycle to affect the eastern margin of North America began in the Triassic with the onset of Atlantic rifting. By this time, however, the Anadarko Basin was located far inboard of the continental margin, and does not appear to have been affected. The most recent structural activity within the basin involves minor reactivation of normal faults that may have occurred during the Jurassic, Cretaceous, and Holocene (Perry, 1989).

As previously mentioned, the Wichita Mountains are bounded to the northeast by the Wichita fault system (fig. 3). Brewer and others (1983) reported that deep reflection seismic profiles across the Anadarko Basin and Wichita Mountains image a series of thrust faults that dip 30° to 40° toward the southeast, and accommodated 9.3 ± 3.1 miles of crustal shortening. This amount of shortening supports the idea that subsidence of the Anadarko Basin was at least partially related to hanging-wall crustal loading (Brewer and others, 1983). In addition to dip-slip motion along the Wichita fault system, there is considerable evidence based upon offset fold hinges and isochores that left-lateral strike slip motion may also have occurred. McConnell (1989) proposed that as much as 7.5 miles of left-lateral motion occurred along the Mountain View fault (fig. 3), and that this supports the arguments put forth by Kluth and Coney (1981) that intracratonic uplifts related to the Ouachita-Marathon orogeny were caused by reactivated slip on faults bounding basement-cored uplifts.

Geodynamic calculations discussed by Garner and Turcotte (1984) led to the suggestion that formation of the Anadarko Basin can best be modeled in terms of elastic flexure of the lithosphere. Under this scenario, compressional forces related to the Ouachita-Marathon orogeny did not cause basinal subsidence. Rather, Garner and Turcotte (1984) argued that compression was caused by flexure-related subsidence of the Anadarko Basin. Given the large amounts of compression accommodated by the Mountain View fault system, it seems likely that formation of the Anadarko Basin was caused by a combination of thrust-loading and flexure-related subsidence.

Stratigraphic Overview

Although a detailed stratigraphic description of the rocks within the Anadarko Basin is beyond the scope of this report, it is important to summarize the key lithologic characteristics of the units shown in the interpretation of the composite seismic line and the structural model (discussed in subsequent sections). A simplified stratigraphic column for the northern Anadarko Basin is shown in figure 4. This study adopts the commonly used stratigraphic nomenclature established for the northern part of the basin, as more well control was available for the northern parts of the composite seismic line. The Anadarko Basin contains too many stratigraphic units to incorporate all into a

regional seismic interpretation and structural model. Therefore, stratigraphic picks on the seismic lines were made for key units based in part on available well control along the seismic lines. The units highlighted in red (fig. 4) were used in the seismic interpretation and structural model. For a more complete stratigraphic section for the Anadarko Basin, see Higley and Gaswirth (2014). Table 1 provides a list of codes for the formation tops identified in the selected wells; the names of some of these tops appear in the following stratigraphic summary. The subsequent paragraphs describe key lithologic features of only the units that are picked on the composite seismic line and incorporated into the structural restoration.

Cambrian and Ordovician Rocks

The oldest unit identified in the seismic interpretation is the Cambrian-Ordovician Arbuckle Group (fig. 4). It consists of shallow-water marine carbonate mudstones and secondary dolomites that reach thicknesses of $\approx 8,000$ ft. (Ball and others, 1991), and forms a significant petroleum reservoir with production primarily from porous dolomite zones (Johnson, 1989). The unconformably overlying Middle Ordovician Simpson Group comprises shallow-water marine limestones, sandstones, and shales (Schramm, 1964). The next overlying Viola Group is a cherty, dolomitic limestone (Bornemann and Doveton, 1983), and the uppermost Ordovician unit is the Sylvan Shale, which is fissile dark green to brown silty marine shale that contains thin intervals of dolomitic sandstone (Huffman, 1953).

Silurian, Devonian, and Mississippian Rocks

Silurian and Lower Devonian rocks of the Anadarko Basin belong to the Hunton Group (fig. 4), which consists of a sequence of limestones and dolomites (Kopaska-Merkel and Friedman, 1989). A significant regional unconformity related to a major sea level low-stand separates the Hunton Group from the overlying Woodford Shale (Kuykendall and Fritz, 1993). The Woodford Shale, which includes the basal informal Misener sand, is one of the Anadarko Basin's major source rocks. The formation is a dark gray to black organic-rich siliceous shale (Kuykendall and Fritz, 1993). Overlying the Woodford Shale are Mississippian carbonates of the Kinderhookian, Osagean, and Meramecian Series. The informal Meramec lime is a thick unit of argillaceous to silty micritic limestone, with higher energy deposits increasing toward the north (Bokman, 1954; Harris, 1975). The Meramec lime is represented in the seismic interpretation by the Goddard Shale (table 1), which is a time equivalent unit (Higley and Gaswirth, 2014) from the southern Anadarko Basin. The youngest Mississippian unit identified in the seismic interpretation is the informal Britt sand (fig. 4), which is part of the Chesterian Series. The Britt sand is predominantly a quartzarenitic to subarkosic sandstone (Andrews and others, 2001). Unconformities within and at the top of the Chesterian Series are products of the onset of the Wichita orogeny.

Table 1. Lithology codes and corresponding stratigraphic units for formation tops shown in figures 15, 16, and 17.

Lithology code	Corresponding stratigraphic unit (see fig. 4)
RSPG	Rush Springs Formation (upper part of the Whitehorse Group) (Higley and Gaswirth, 2014)
WLNG	Wellington Formation
CHSE	Chase Group
CCGV	Council Grove Group
ADMR	Admire Group
WBNS	Wabaunsee Group
TOPK	Topeka Limestone
TNKW	Tonkawa sand (upper part of the Douglas Group) (Higley and Gaswirth, 2014)
CGGV	Cottage Grove Sandstone (lower part of the Lansing Group)
HGSR	Hogshooter Limestone
CCKB	Checkerboard Limestone
MRMN	Marmaton Group
RDFK	Taft Sandstone (also called the Red Fork sand) (Higley and Gaswirth, 2014)
MRRW	Morrow Formation
BRTT	Britt sand
GDRD	Goddard Shale (same age as the Meramec lime) (Higley and Gaswirth, 2014)
WDFD	Woodford Shale
HNTN	Hunton Group
SLVN	Sylvan Shale
VIOL	Viola Group

Pennsylvanian Rocks

The oldest Pennsylvanian unit identified in the seismic interpretation is the Morrow Formation (fig. 4). It consists mostly of shale deposited during a marine transgression; interbedded sandstones were deposited during brief regressions (Ball and others, 1991). Following the climax of the Wichita orogeny during Atokan time, rocks of the Cherokee Group, including the Taft Sandstone, were deposited. The Taft Sandstone is also known informally as the Red Fork sand (Higley and Gaswirth, 2014; table 1), which comprises mainly shale interbedded with thin limestone and calcareous siltstone (Mannhard and Busch, 1974). The overlying Marmaton Group consists of limestones interbedded with shales and a coarsening-upward sequence of mudstones and sandstones (Rascoe, 1962; Hentz, 1994). Missourian rocks of the Kansas City Group (including the Checkerboard and Hogshooter Limestones) and the Lansing Group (including the Cottage Grove Sandstone) are predominantly dark gray shales interbedded with a few sandstones and thin, dense limestones (Rascoe, 1962). The Douglas Group at the base of the Virgilian Series, which includes the informal Tonkawa sand (Higley and Gaswirth, 2014; table 1), is mostly red and gray sandy shales and thin, dense limestones (Rascoe, 1962). The Topeka Limestone is a massive shelfal carbonate that grades into a sequence of

silty shales and thin limestones and sandstones in deeper parts of the Anadarko Basin (Rascoe, 1962). The Wabaunsee Group, which consists of shelfal limestones and calcareous shales in the deep basin (Rascoe, 1962), occupies the top of the Pennsylvanian section.

Permian Rocks

Rocks of the Wolfcampian Series (fig. 4) are primarily shallow marine limestones and shales. The basal Admire Group and overlying Council Grove Group are made up of massive marine limestones and shales; in the northern part of the basin, there are nonmarine red silty shales and siltstones (Rascoe and Adler, 1983). The Chase Group is mostly interbedded limestones and shales; in western parts of the basin, the group grades abruptly into red silty sandstones and shales (Rascoe, 1962). The only Leonardian unit identified in the seismic interpretation is the Wellington Formation, which consists of interbedded alluvial and deltaic sandstones and shales (Johnson and others, 1988). The youngest unit identified in the seismic interpretation is the Guadalupian Whitehorse Group (fig. 4), which includes the Rush Springs Formation (Higley and Gaswirth, 2014; table 1). The Whitehorse Group consists of red sandstones and thin anhydrites (Johnson and others, 1988).

2D Reflection Seismic Datasets Available to the U.S. Geological Survey

As part of the 2010 Anadarko Basin petroleum resource assessment, the USGS licensed five seismic lines from Seismic Exchange, Inc., that total approximately 137 line miles (220 km; fig. 2). The lines were acquired by four different companies between 1978 and 1985, using widely varying data acquisition (recording) parameters. The line names, locations where recorded (county names), year purchased by the USGS, and line lengths are given in table 2. Relevant recording

parameters for each of the lines are given in table 3. Note that because of the proprietary nature of the seismic data, the lines shown in figure 2 are given general names (Line A, Line B, Line C, Line D, and Line E), rather than the original line names provided by Seismic Exchange, Inc.

The data were reprocessed by the USGS between 2008 and 2010 using Halliburton's ProMAX seismic data processing software. Lines B, D, and E were completely reprocessed by the USGS, beginning with the field data, through the point of migrated depth. Line A was reprocessed beginning with the field data through detailed velocity analysis, and the resulting velocity model was used to convert the industry-migrated data

Table 2. Seismic line names, counties and states where seismic lines were recorded, the year the USGS purchased licenses for the data, and the lengths of each line. Seismic data are owned or controlled by Seismic Exchange, Inc.; interpretation is that of the U.S. Geological Survey.

Line name	Counties and States where recorded	Year licensed	Line lengths in miles/kilometers
Line A	Beckham & Roger Mills, OK; Wheeler, TX	2009	17.0/27.4
Line B	Woodward, Ellis, & Dewey, OK	2007	31.2/50.2
Line C	Kiowa & Washita, OK	2009	16.8/27.0
Line D	Washita & Custer, OK	2007	34.7/55.8
Line E	Blaine, Caddo, Major, & Washita, OK	2007	36.9/59.3

Table 3. Data acquisition parameters for the five seismic lines used in this study. Seismic data are owned or controlled by Seismic Exchange, Inc.; interpretation is that of the U.S. Geological Survey.

Recording parameter	Line name and associated parameter values				
	Line A	Line B	Line C	Line D	Line E
Year recorded	1978	1985	1980	1980	1982
Recorded by	Seismic Resources, Inc.	Western	Seismic Resources, Inc.	Milestone	Digicon
Energy source type	Dynamite	Vibroseis	Dynamite	Dynamite	Dynamite
Source depth	150 feet 45.7 meters	n/a	150 feet 45.7 meters	100–260 feet 30.5–79.2 meters	160 feet 47.8 meters
Charge size	25–40 pounds 11.4–18.2 kilograms	n/a	50 pounds 22.7 kilograms	5–40 pounds 2.3–18.2 kilograms	10–40 pounds 4.5–18.2 kilograms
Sweep frequencies/ length	n/a	10–85 hertz/ 10 seconds	n/a	n/a	n/a
Source pattern	Single hole	3 or 4 Vibrators	Single hole	Single hole	Single hole
Source interval(s)	440 feet 134.1 meters	165 feet 50.3 meters	440 feet 134.1 meters	240 feet 73.1 meters	440 feet 134.1 meters
Number of receiver channels	96	96	96	120	96
Receiver spread configuration	Symmetrical split spread	Symmetrical split spread	Symmetrical split spread	End-on	Symmetrical split spread
Near/far source-receiver offset	220/10,560 feet 67/3,219 meters	660/8415 feet 201.2/2,565 meters	165/5170 feet 50.3/1,578 meters	120/14,440 feet 36.5/4,386 meters	110/10,340 feet 33.5/3,152 meters
Receiver group interval	220 feet 67 meters	165 feet 50.3 meters	110 feet 33.5 meters	120 feet 36.5 meters	220 feet 67 meters
Nominal common depth point fold	24	48	12	30	24

to depth. Line C was not reprocessed, but the stacking velocities were analyzed, edited, smoothed, and used to convert the industry-migrated data to depth. During reprocessing, the following generalized sequence of processing steps was used.

Before stacking: amplitude scaling, single or multiple window spiking deconvolution, datum statics using smoothed surface elevations, velocity analysis [root-mean-square (RMS) velocities determined directly from the seismic data], surface-consistent residual statics, a second velocity analysis, second pass of residual statics if necessary, normal moveout correction using the stacking velocities, and common depth point (CDP) stacking.

After stacking: shift both the seismic data and the velocity fields to a horizontal datum, automatic gain control scaling, bandpass filter, post-stack time migration using a smoothed version of the stacking velocity field, and depth conversion using the same smoothed velocity field. With the exception of Line C as explained below, the stacking velocities were determined directly from the seismic data using conventional velocity analysis applied at points along the lines where there was good signal-to-noise ratio. Two passes

of velocity analyses were performed, one before and one after residual statics analysis. Velocity functions were picked manually from the interactive onscreen analysis display, except for the second pass on Line D, where an automated velocity picking routine was used. This method used the manually picked velocities from the first pass as a guide function. Velocity functions were picked at a 25-CDP interval, and were constrained to -5 percent to +10 percent about the guide function at the surface, and $\pm 10\%$ about the guide function at 2,500 milliseconds (ms). This method was successful in producing a detailed velocity field for stacking. However, the stacked image produced using the automated velocity picks was only minimally improved over that of the manually picked velocity model. This velocity model was smoothed (201 CDPs horizontal; 250 ms vertical smoothing operator), and was used for migration and depth conversion (fig. 8). For Line C, stacking velocities were provided with the industry-migrated data. These velocities were analyzed and edited to ensure that the interval velocities were geologically reasonable, and then a smoothed version of those velocities was used for migration and depth conversion.

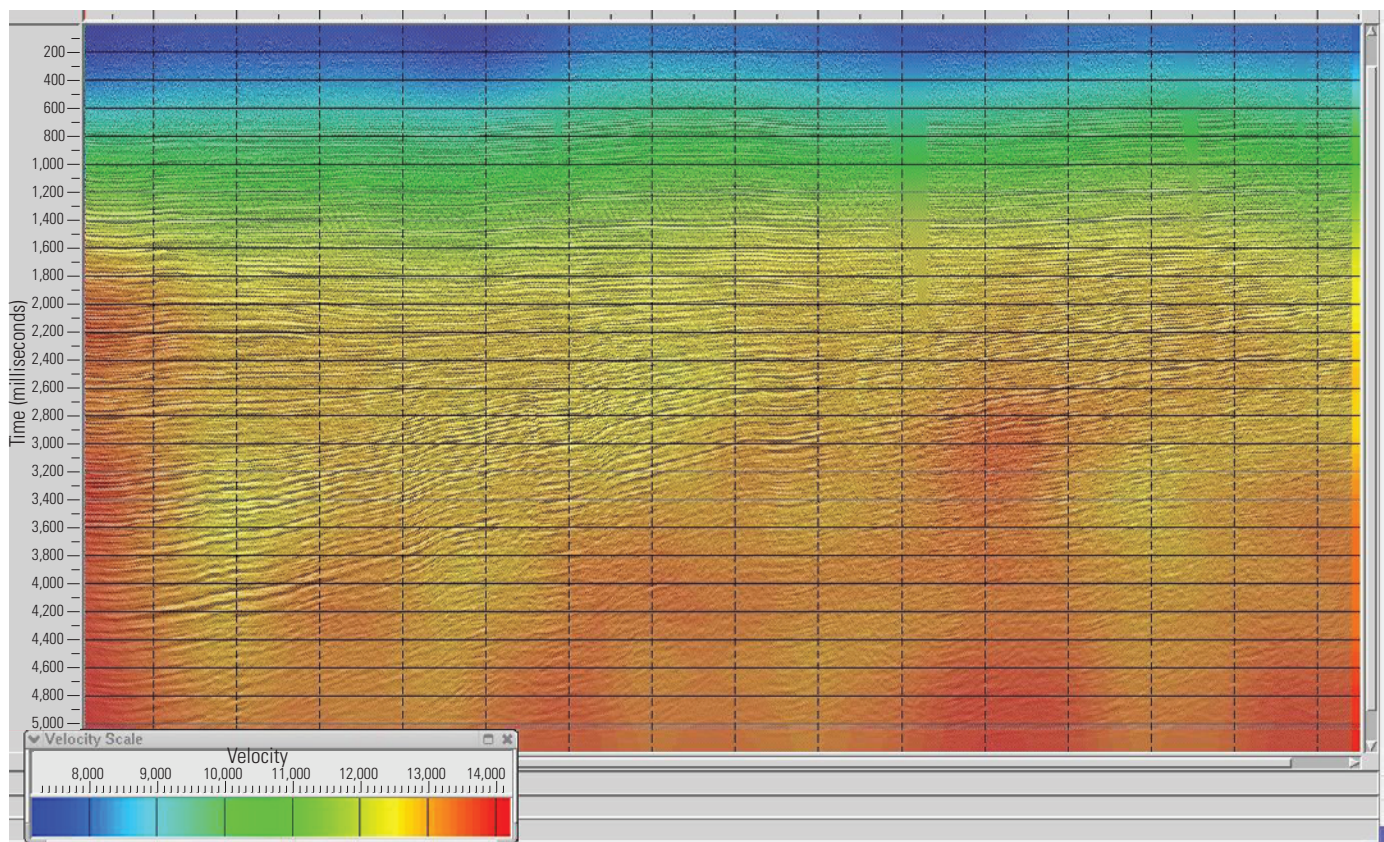


Figure 8. Root mean square velocity model used to migrate and convert seismic Line D. Velocities were determined using an automated velocity picking algorithm, and subsequently smoothed using a 201 common depth point horizontal, and 250-millisecond vertical, smoothing operator. A color bar illustrating the velocity scale is also shown. Seismic data are owned or controlled by Seismic Exchange, Inc.; interpretation is that of the U.S. Geological Survey.

2D Reflection Seismic Data Interpretation

General Description of the Seismic Lines

Although the seismic lines were all acquired almost 30 years ago, key stratigraphic and structural features of the Anadarko Basin can be seen in the images. Figures 9–13 show uninterpreted depth sections for Line A, Line B, Line C, Line D, and Line E, respectively. All lines are shown at the same scale, with the vertical (depth) and horizontal (miles along the surface) axes equal. All lines are also shown with identical red to black color bars, where red colors represent amplitude troughs and black colors represent amplitude peaks. A brief qualitative description is given in the following paragraphs for each of the seismic lines.

Line A (fig. 9) crosses the southern boundary of the Anadarko Basin onto the Wichita uplift (fig. 3). Non-continuous reflectors with apparent northeast dips can be seen at shallow depths along the southwestern portion of the line. The lack of continuous reflectors at the line's southwestern most edge likely shows the presence of Precambrian basement rocks of the Wichita uplift in the hanging-wall of the Mountain View fault system. The subparallel reflectors that reach depths of $\approx 30,000$ ft and extend across the northeastern two-thirds

of the line are caused by Cambrian-Permian rocks of the Anadarko Basin. The axis of the basin lies between about three to five miles from the southwest edge of the seismic line, depending upon the stratigraphic level.

Line B (fig. 10) shows subparallel, largely continuous reflectors with apparent gentle southwest dips. It is possible to trace many of the shallow reflectors (above 15,000 ft at the southwest edge of the line) along the entire 31.2-mile length of the seismic line. The southwestern expansion of the Cambrian-Permian stratigraphic section can be clearly seen. For example, the prominent reflectors at depths of approximately 2,500 ft and 7,500 ft at the northeastern edge of the line reach depths of approximately 3,500 ft and 12,000 ft at the southwestern edge of the line.

Line C (fig. 11) is similar in many ways to Line A, in that it spans the boundary between the Anadarko Basin and the Wichita uplift. Although the basin-bounding thrust faults are not directly imaged, it is possible to infer the presence of at least two faults. The Mountain View fault system likely exists at the southwest edge of the line, and is responsible for elevating basement rock characterized by non-continuous reflectors. The obvious monoclinical flexure in the middle of the line may be caused by the Cordell fault (fig. 3). Although the southwestern third of the line is poorly imaged, the fold geometry is similar to that described for many Laramide basement-cored uplifts (Erslev, 1991; Brandenburg and others, 2012). Shallow

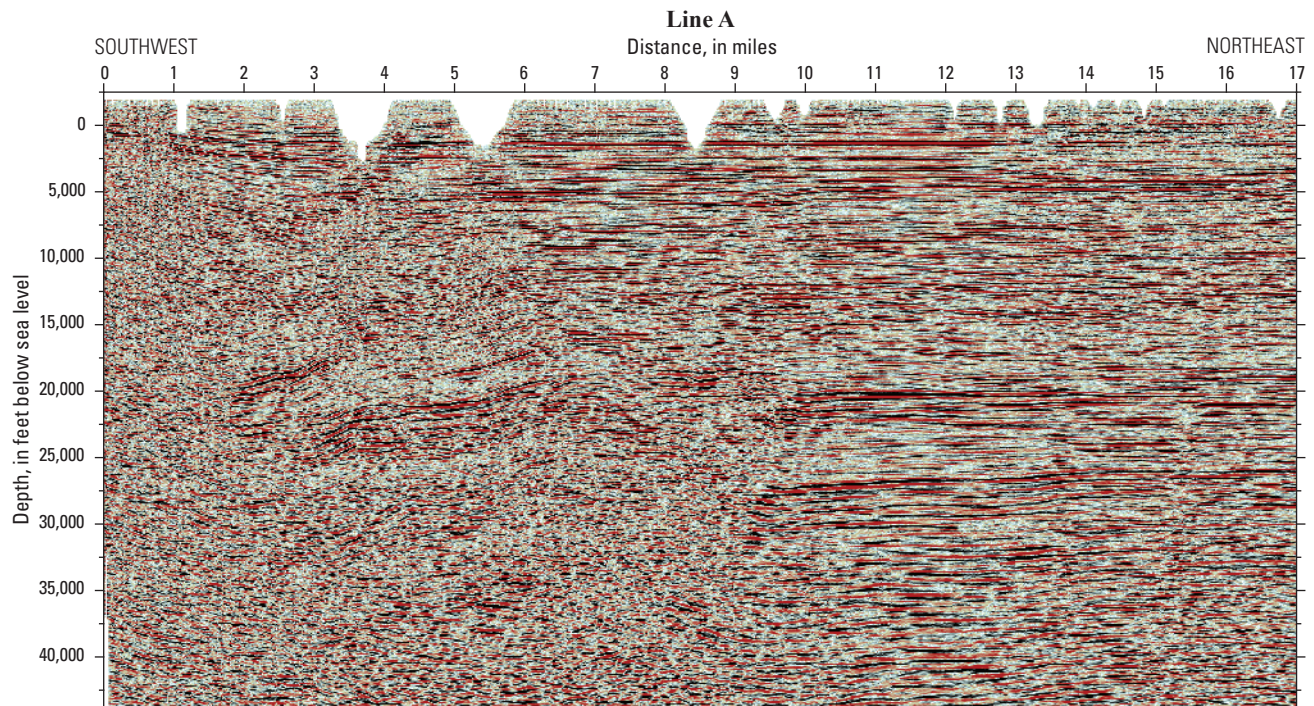


Figure 9. Uninterpreted seismic Line A. Location of line is shown in figure 2. Horizontal and vertical scales are equal. Black colors are amplitude peaks; red colors are amplitude troughs. Seismic data are owned or controlled by Seismic Exchange, Inc.

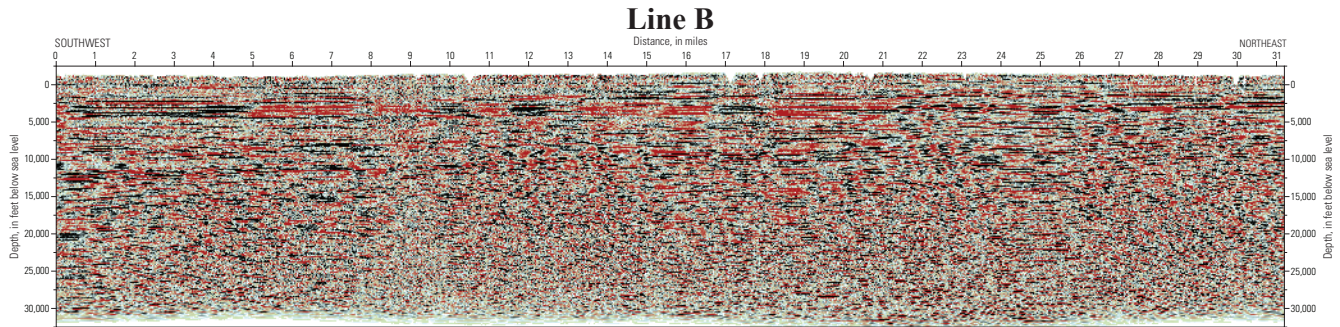


Figure 10. Uninterpreted seismic Line B. Location of line is shown in figure 2. Horizontal and vertical scales are equal. Dark black colors are amplitude peaks; dark red colors are amplitude troughs. Seismic data are owned or controlled by Seismic Exchange, Inc. Figure 10 is oversized. Click on the thumbnail to view the enlarged version.

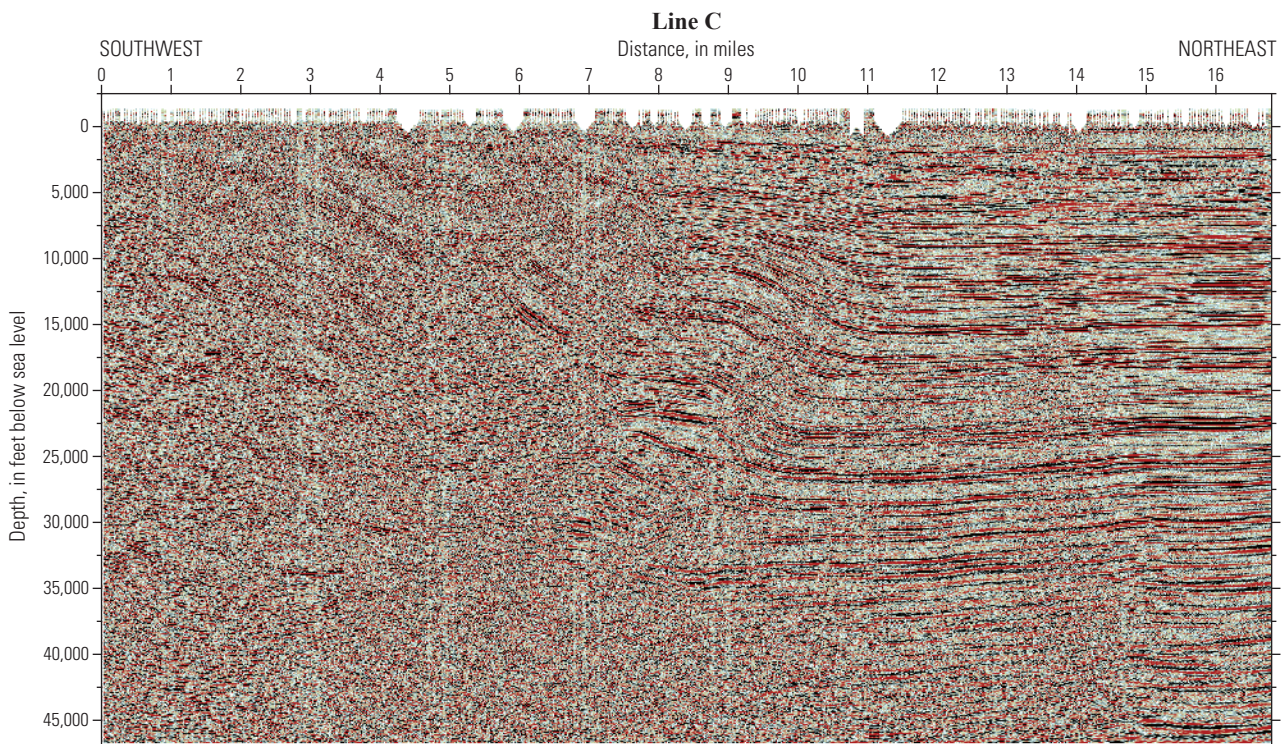


Figure 11. Uninterpreted seismic Line C. Location of line is shown in figure 2. Horizontal and vertical scales are equal. Dark black colors are amplitude peaks; dark red colors are amplitude troughs. Seismic data are owned or controlled by Seismic Exchange, Inc.

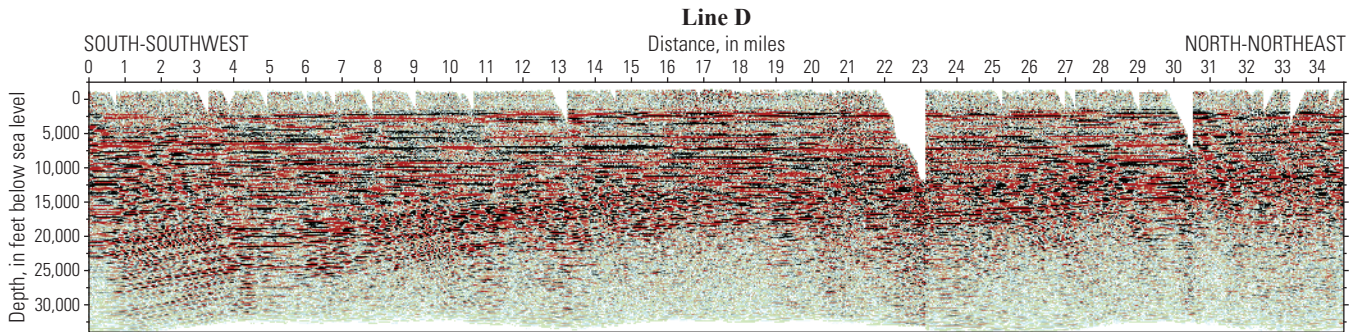


Figure 12. Uninterpreted seismic Line D. Location of line is shown in figure 2. Horizontal and vertical scales are equal. Dark black colors are amplitude peaks; dark red colors are amplitude troughs. Seismic data are owned or controlled by Seismic Exchange, Inc. Figure 12 is oversized. Click on the thumbnail to view the enlarged version.

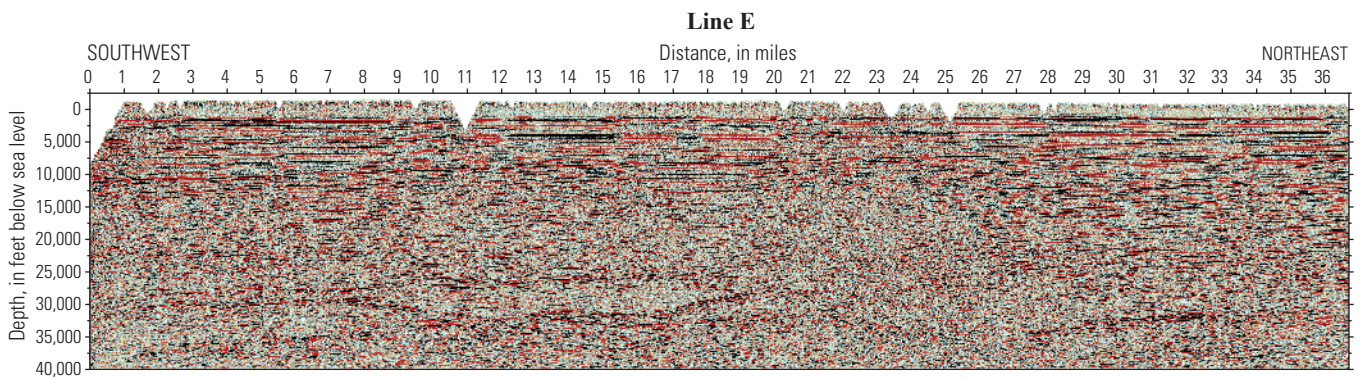


Figure 13. Uninterpreted seismic Line E. Location of line is shown in figure 2. Horizontal and vertical scales are equal. Dark black colors are amplitude peaks; dark red colors are amplitude troughs. Seismic data are owned or controlled by Seismic Exchange, Inc. Figure 13 is oversized. Click on the thumbnail to view the enlarged version.

reflectors that have apparent dips toward the northeast along the southwestern third of the line are generally poorly imaged and are difficult to track. However, stratigraphic on-lap and angular truncation of reflectors can be seen at depths above 5,000 ft from six to eight miles from the southwest edge of the seismic line. Depending upon the stratigraphic level, the axis of the basin is between approximately 8 and 12 miles from the southwestern edge of the seismic line. Northeast of the basin's axis, subparallel reflectors made by Cambrian-Permian rocks are well-imaged and are easy to track.

Line D (fig. 12) is characterized by well-imaged, subparallel reflectors with apparent south-southwest dips. As with Line B, it is possible to track numerous reflectors across the entire 34.7-mile-long seismic line. At the resolution and scale of the image, reflectors (those above approximately 27,500 ft at the south-southwest edge of the image) do not appear to be offset by faults. The south to southwestern expansion of the Cambrian-Permian section is well-imaged by this line;

reflectors at depths of approximately 12,500 ft at the north-northeast edge of the line reach depths of approximately 27,500 ft at the south-southwest edge of the line.

Line E (fig. 13) contains a well-imaged section down to approximately 15,000 ft depth at the southwest edge of the line and 10,000 ft at the northeast edge. As with previously described lines, it is possible to trace numerous individual reflectors across the entire 36.9-mile length of the seismic image without encountering any offsets because of faulting. Reflectors have gentle apparent dips toward the southwest and show the thickening of the Cambrian-Permian section toward the basin's axis. Layered intrusives possibly related to the southern Oklahoma aulacogen may be visible between depths of 30,000 and 35,000 ft along the southwestern half of the seismic line.

Because of their proximity to each other, Lines C, D, and E were selected for a more detailed seismic interpretation. These three lines are henceforth collectively referred to as the Anadarko "composite seismic line." Interpretation of the composite seismic line was guided by formation tops information from 18 selected wells (fig. 14) that were projected orthogonally onto the line of section from distances of up to 7.5 miles off the composite seismic line. These wells are a subset of more than 220 wells across the Anadarko Basin Province that contain edited formation tops. A detailed discussion of the numerous data sources and the methodology behind picking these formation tops is given in Higley and others (2014) and references therein.

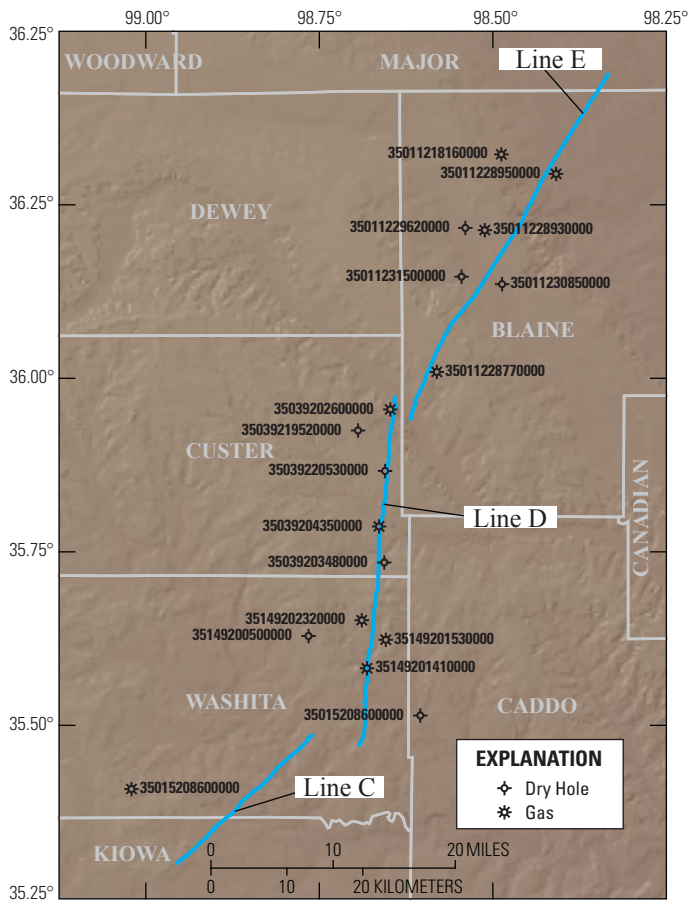


Figure 14. Map showing the location of wells used to aid in the interpretation of the composite seismic line. Oklahoma counties are shown in gray. The segments of the composite seismic line are shown in blue. American Petroleum Institute well numbers are given.

Seismic Interpretation of the Anadarko Composite Seismic Line

Interpretations for Line C, Line D, and Line E are shown in figures 15, 16, and 17, respectively. The lines are all shown at the same scale, and the vertical (depth) and horizontal (distance along the surface) axes are identical. The projected location of the wells and relevant formation tops (table 1) are also shown.

Interpretation of Lines D and E is facilitated by the ease with which numerous individual reflectors can be traced across the entire length of the lines. No faults were interpreted to be present on these two lines; however, if present, they were either not imaged by the seismic data or are of a subseismic scale. Formation tops from the 17 wells projected onto these two seismic lines permits identification of 20 horizons; the only two horizons for which well control is not available are the Simpson and Arbuckle Groups. On Line E (fig. 17), the top of the Simpson Group was placed at the next prominent reflector below the top of the Viola Group in well 35011230850000, which gives an apparent thickness for the Viola Group at that location of ≈ 460 ft. The top of the Arbuckle Group was placed at the next prominent reflector below the top of the Simpson Group at the same location, which yields an apparent thickness for the Simpson Group of ≈ 750 ft. Although these two

horizons probably do not represent the actual tops of the Simpson and Arbuckle Groups, they are likely to be close. Evidence in support of this comes from the combined thickness of the Viola and Simpson Groups at the southwestern edge of the interpretation on Line C. Johnson and others (1988) suggested that the maximum combined thickness of the two groups in southern Oklahoma is in excess of $\approx 2,500$ ft; the maximum thickness of the two groups at the southwestern edge of the interpretation is $\approx 2,800$ ft.

Interpretation was only done for the northeastern half of Line C (fig. 15), because of the poor quality of the seismic data combined with a lack of well control and the complex geometries of the frontal portion of the Wichita uplift in the southwestern part. McConnell (1989) provided examples of complex compressional geometries at the northern edge of the Wichita uplift. Although locations for thrust faults of the Mountain View fault system and the Cordell fault (fig. 3) could have been hypothesized, available data do not permit determination of the hanging-wall and footwall cutoff relations, and thus constrain either the magnitude or timing of displacement along the faults.

Structural Restoration of the Anadarko Composite Seismic Line

A structural restoration of the composite seismic line was built using Midland Valley’s 2DMove software. The restoration shown in figure 18 details 22 stages corresponding to each of the interpreted stratigraphic units (fig. 4) described in the preceding sections. As with all other figures that show the seismic lines and interpretations, the horizontal and vertical scales in each panel of figure 18 are identical.

The restoration was pinned at the northeast edge of the composite seismic line, and all horizons were restored to a horizontal surface at an elevation of the present sea level. The primary restoration algorithm used within 2DMove was “Flexural Slip Unfolding.” The flexural slip algorithm was used for the following reasons: (1) it maintains the line length of the template horizon (the template horizon is the horizon that is being restored to the horizontal surface) in the direction of unfolding; (2) it maintains the orthogonal bed thickness between the template horizon and all other passive horizons

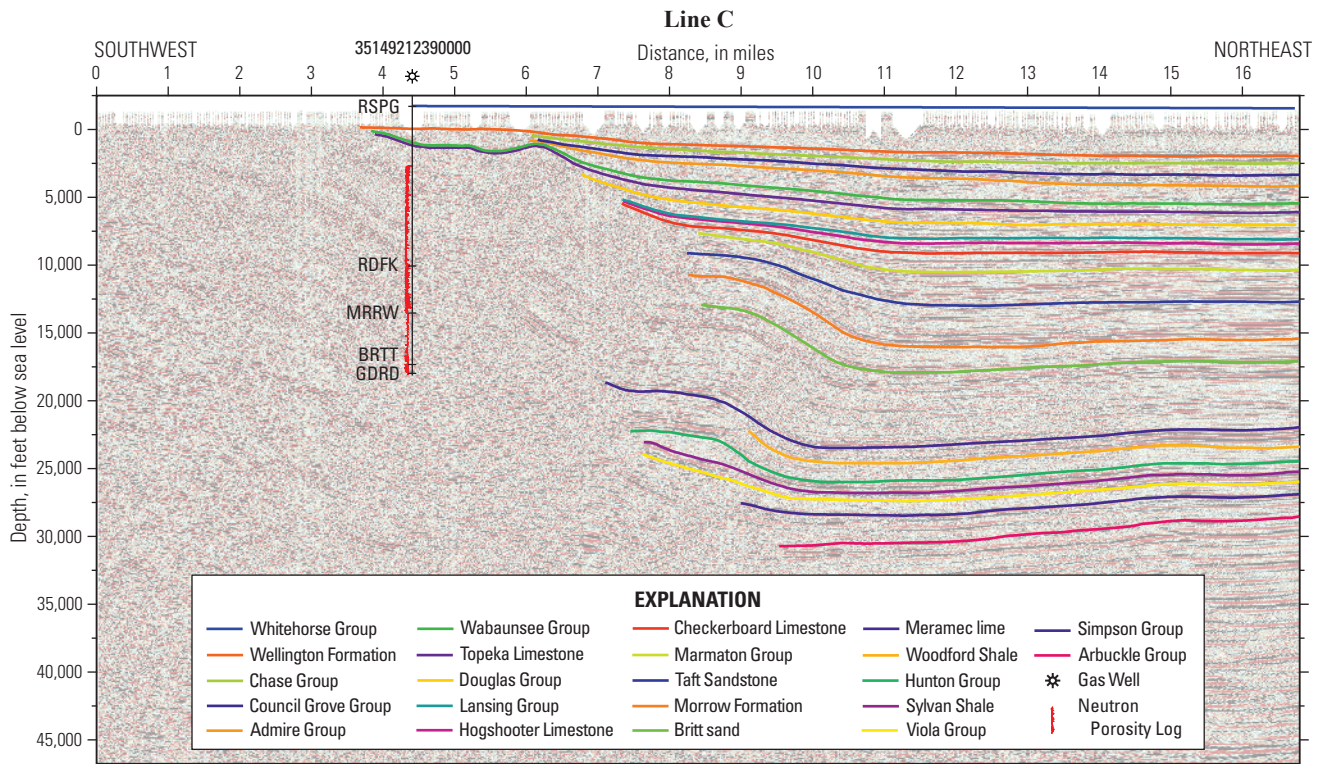


Figure 15. Interpreted seismic Line C. Location of line is shown in figure 2. Horizontal and vertical scales are equal. Dark black colors are amplitude peaks; dark red colors are amplitude troughs. Well symbols are the same as those used in fig. 14. American Petroleum Institute well numbers are indicated. Lithology codes for well tops are given in table 1. Seismic data are owned or controlled by Seismic Exchange, Inc.; interpretation is that of the U.S. Geological Survey.

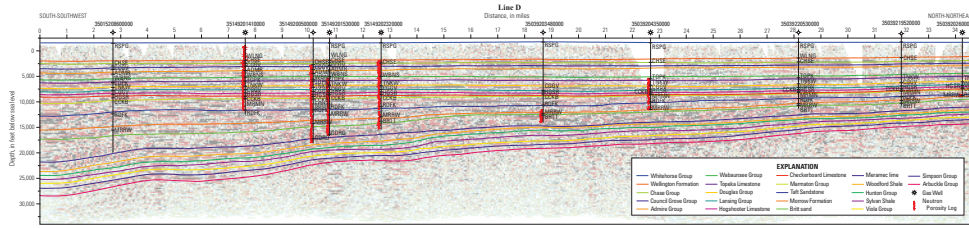


Figure 16. Interpreted seismic Line D. Location of line is shown in figure 2. Horizontal and vertical scales are equal. Dark black colors are amplitude peaks; dark red colors are amplitude troughs. Well symbols are the same as those used in fig. 14. American Petroleum Institute well numbers are indicated. Lithology codes for well tops are given in table 1. Seismic data are owned or controlled by Seismic Exchange, Inc.; interpretation is that of the U.S. Geological Survey. Figure 16 is oversized. Click on the thumbnail to view the enlarged version.

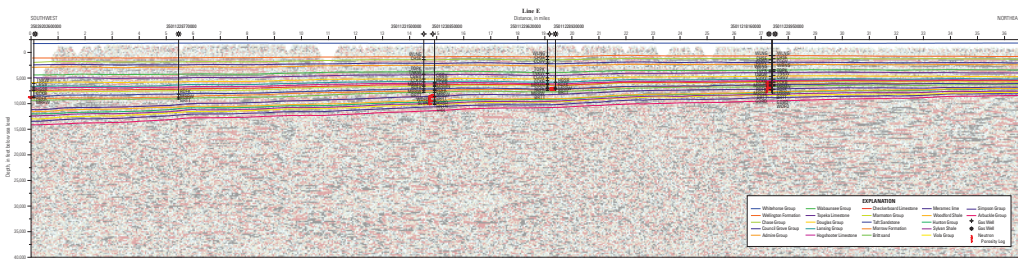


Figure 17. Interpreted seismic Line E. Location of line is shown in figure 2. Horizontal and vertical scales are equal. Dark black colors are amplitude peaks; dark red colors are amplitude troughs. Well symbols are the same as those used in figure 14. American Petroleum Institute well numbers are indicated. Lithology codes for well tops are given in table 1. Seismic data are owned or controlled by Seismic Exchange, Inc.; interpretation is that of the U.S. Geological Survey. Figure 17 is oversized. Click on the thumbnail to view the enlarged version.

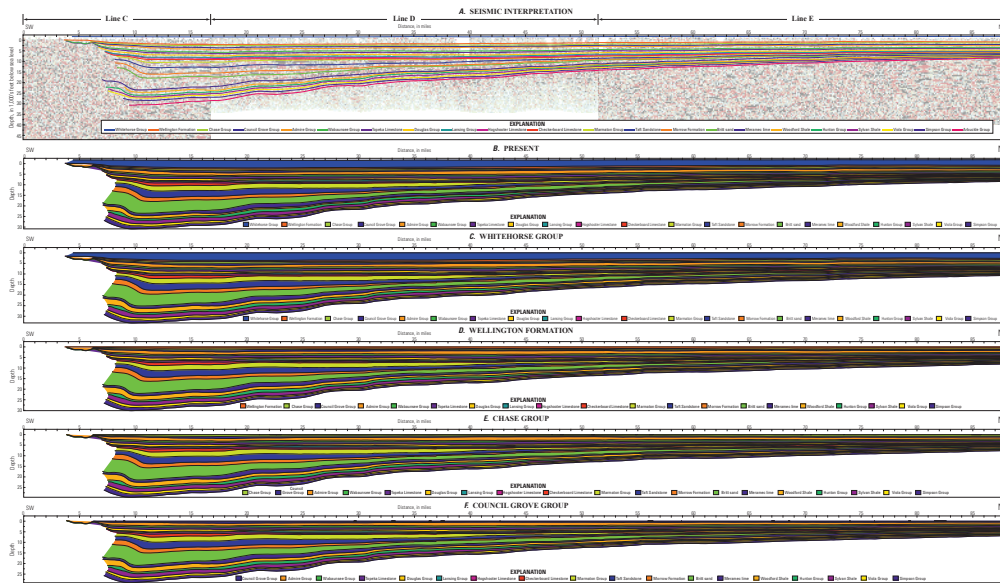


Figure 18. Structural restoration showing individual restoration stages. Depth in each stage is shown in thousands of feet below sea level; horizontal distance is given in miles from the southwestern edge of seismic Line C (no vertical exaggeration). Seismic data are owned or controlled by Seismic Exchange, Inc.; interpretation is that of the U.S. Geological Survey. Figure 18 is oversized. Click on the thumbnail to view the enlarged version.

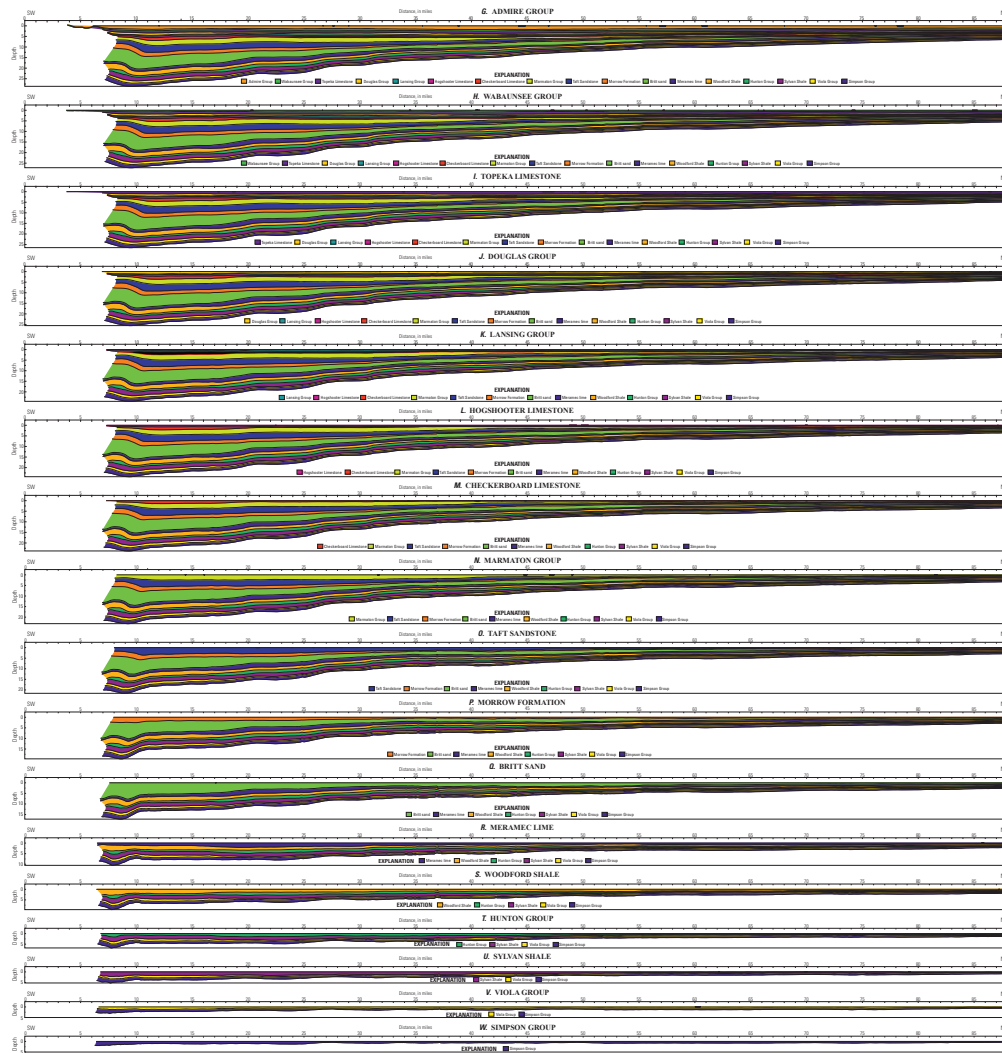


Figure 18. Structural restoration showing individual restoration stages. Depth in each stage is shown in thousands of feet below sea level; horizontal distance is given in miles from the southwestern edge of seismic Line C (no vertical exaggeration). Seismic data are owned or controlled by Seismic Exchange, Inc.; interpretation is that of the U.S. Geological Survey. Figure 18 is oversized. Click on the thumbnail to view the enlarged version.—Continued

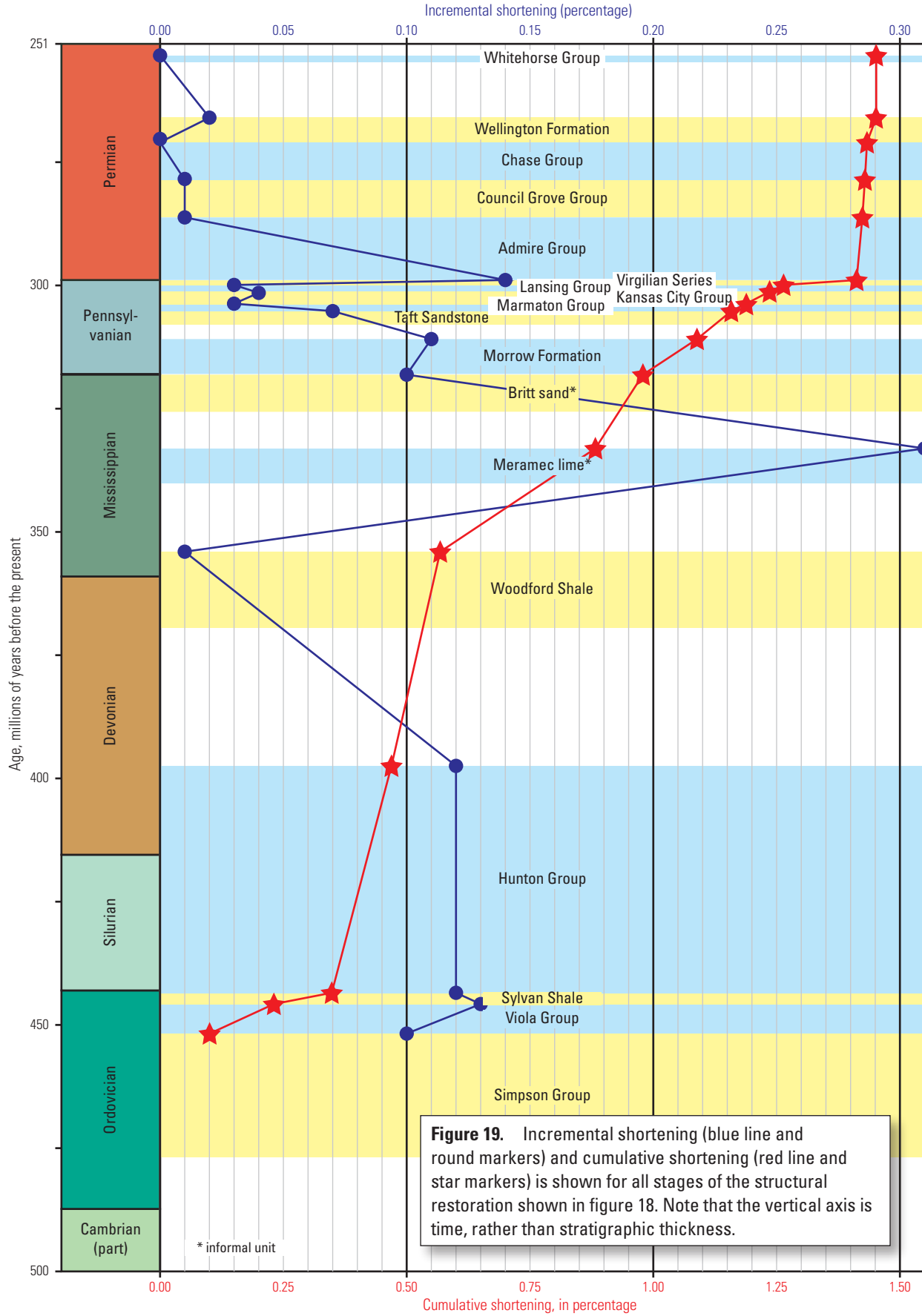


Figure 19. Incremental shortening (blue line and round markers) and cumulative shortening (red line and star markers) is shown for all stages of the structural restoration shown in figure 18. Note that the vertical axis is time, rather than stratigraphic thickness.

(passive horizons are the horizons below the template horizon); and (3) it maintains area of the fold and model. Additionally, the flexural slip algorithm is an appropriate choice inasmuch as the composite seismic line is roughly orthogonal to the northern flank of the Wichita uplift; the dominant stresses responsible for the creation of the Wichita uplift and the Anadarko Basin were therefore roughly aligned with the northeast-southwest orientation of the composite seismic line.

Each stage of the restoration (fig. 18 *B–W*) shows the 2D geometry that may have existed at the end of deposition of each interpreted lithologic unit. The restoration shows that in deeper parts of the basin, between approximately 7 and 45 miles from the southwest end of the model, subtle structural relief developed along most of the horizons soon after the deposition of individual units. For example, a broad fold had developed in the Meramec lime about 20 miles from the southwestern end of the model (fig. 18 *Q* and *R*) by the end of deposition of the Britt sand. Some of the shorter wavelength features, such as the narrow fold at about 37 miles from the southwest end of the model (fig. 18 *Q–W*), are likely artifacts of the restoration.

As previously mentioned, the restoration is pinned at the northeast edge of the composite seismic line. Relative to the margin of the Ouachita orogeny, this location is within the stable North American craton. Progressive shortening of the restoration can therefore be seen by individual horizons lengthening in a southwesterly direction, in reverse chronological order. During the time represented by the deposition of the Simpson Group through the Whitehorse Group, the cumulative amount of shortening along the cross-section is 1.45 percent. Although this is not a large amount of shortening, it is important to recognize that it took place entirely within the footwalls of the thrust faults that separate the Wichita uplift and the Anadarko Basin. McConnell (1989) estimated that approximately 6.7 miles of reverse-slip occurred on these frontal faults. The magnitude of Ordovician through Permian shortening is shown in figure 19, which displays both the incremental (blue line and round markers) and cumulative (red line and star markers) shortening percentages through time. For example, by the end of deposition of the Viola Group, the underlying Simpson Group rocks had been shortened by 0.10 percent; by the end of deposition of the Britt sand, the underlying Meramec lime had been shortened by 0.31 percent. The cumulative shortening line reveals that most of the shortening within the basin was during Mississippian and Pennsylvanian time. Since deposition of the Virgilian Series, almost no shortening has occurred. Significant tectonic shortening during the Permian is absent, so accommodation space for Permian rocks was likely created by isostatic subsidence of the basin. Calculation of the relatively minor amount of shortening experienced by rocks within the Anadarko Basin to the north of the Mountain View fault system supports the interpretation (figs. 15, 16, and 17) that no faults are present along the seismic lines, at least none that is visible at the scale of the seismic data available for this study. The key point is that shortening within the Anadarko Basin was primarily accommodated by minor folding, rather than faulting.

Summary

The structural evolution of the Anadarko Basin Province was affected by tectonic processes associated with two complete Wilson cycles that affected the eastern margin of North America. The first Wilson cycle, which involved the creation and subsequent breakup of the Rodinian supercontinent, accounts for the consolidation of basement rock beneath the Anadarko Basin Province and the emplacement of the southern Oklahoma aulacogen. The second Wilson cycle, which involves the formation and breakup of Pangaea, controlled the depositional environments of the Anadarko Basin's more than 40,000 feet of Cambrian through Permian sediments and the geometry of the basin's current geometry. The geometry of each of the major structural elements was partially inherited from prior tectonic and structural events.

The U.S. Geological Survey licensed and analyzed five two-dimensional reflection seismic lines within the Anadarko Basin. Three of the lines have endpoints that approximately overlap; these were combined into a regional composite seismic line that extends almost 90 miles in a northeast-southwest direction across the basin. A detailed seismic interpretation, based in part on well data, shows relatively undeformed Cambrian through Permian strata that dip toward the southwest into the trough of the Anadarko Basin. The Wichita Mountains structural high and disrupted strata associated with the Wichita fault system can also be seen on the southeastern edge of the composite seismic line. A structural restoration shows the sequential burial of 22 key stratigraphic horizons. At the scale of the available seismic data, there is little visible structural deformation within the Anadarko Basin northeast (in the footwall) of the Wichita fault system.

Acknowledgments

We would like to thank Kristen Marra, Sarah Hawkins, and Dick Keefer for constructive technical reviews of this paper. We also thank Seismic Exchange, Inc., for giving permission to publish the seismic data. Members of the USGS Anadarko Basin assessment team, in particular Debra Higley and Stephanie Gaswirth, provided insightful discussions about the Anadarko Basin, and were a valuable aid in our study.

References Cited

- Andrews, R.D., Hendrickson, W.J., and Smith, P.W., 2001, Regional overview of the Springer gas play, Springer gas play in western Oklahoma: Oklahoma Geological Survey Special Publication 2001-1, p. 1-26.
- Ball, M.M., Henry, M.E., and Frezon, S.E., 1991, Petroleum geology of the Anadarko Basin region, Province (115), Kansas, Oklahoma, and Texas: U.S. Geological Survey Open-File Report 88-450W, 36 p.

- Blakey, R.C., 2011, North American paleogeographic maps, Middle Cambrian (510 Ma): accessed May 4, 2012, at <http://cpgeosystems.com/namC510.jpg>.
- Bokman, J., 1954, Relative abundance of common sediments in Anadarko Basin of Oklahoma: American Association of Petroleum Geologists Bulletin, v. 38, p. 648–654.
- Bornemann, E., and Doveton, J.H., 1983, Lithofacies mapping of Viola Limestone in south-central Kansas, based on wire-line logs: American Association of Petroleum Geologists Bulletin, v. 67, p. 609–623.
- Brandenburg, J.P., Alpak, F.O., Solum, J.G., and Naruk, S.J., 2012, A kinematic trishear model to predict deformation bands in a fault-propagation fold, East Kaibab monocline, Utah: American Association of Petroleum Geologists Bulletin, v. 96, p. 109–132.
- Brewer, J.A., Good, R., Oliver, J.E., Brown, L.D., and Kaufman, L., 1983, COCORP profiling across the southern Oklahoma aulacogen: Overthrusting of the Wichita Mountains and compression within the Anadarko Basin: *Geology*, v. 11, p. 109–114.
- Cardott, B.J., and Lambert, M.W., 1985, Thermal maturation by vitrinite reflectance of Woodford Shale, Anadarko Basin, Oklahoma: American Association of Petroleum Geologists Bulletin, v. 69, p. 1982–1998.
- Erslev, E., 1991, Trishear fault-propagation folding: *Geology*, v. 19, p. 617–620.
- Feinstein, S., 1981, Subsidence and thermal history of southern Oklahoma aulacogen: Implications for petroleum exploration: American Association of Petroleum Geologists Bulletin, v. 65, p. 2521–2533.
- Garner, D.L., and Turcotte, D.L., 1984, The thermal and mechanical evolution of the Anadarko Basin: *Tectonophysics*, v. 107, p. 1–24.
- Gilbert, M.C., 1982, Geologic setting of the eastern Wichita Mountains with a brief discussion of unresolved problems, *in* Gilbert, M.C. and Donovan, R.N., eds., *Geology of the eastern Wichita Mountains*: Oklahoma Geological Survey Guidebook 21, p. 1–30.
- Gilbert, M.C., 1983, Timing and chemistry of igneous events associated with the southern Oklahoma aulacogen, *in* Morgan, P., and Baker, B.H., eds., *Processes of continental rifting*: *Tectonophysics*, v. 94, p. 439–455.
- Gilbert, M.C., 1987, Petrographic and structural evidence from the igneous suite in the Wichita Mountains bearing on the Cambrian tectonic style of the southern Oklahoma aulacogen: *Geological Society of America Abstracts with Programs*, v. 19, p. 152.
- Ham, W.E., 1973, Regional geology of the Arbuckle Mountains, Oklahoma: Oklahoma Geological Survey Special Publication 73–3, 56 p.
- Harlton, B.H., 1963, Frontal Wichita fault system of southwestern Oklahoma: American Association of Petroleum Geologists Bulletin, v. 47, p. 1552–1580.
- Harris, S.A., 1975, Hydrocarbon accumulation in “Meramec-Osage” (Mississippian) rocks, Sooner trend, northwestern Oklahoma: American Association of Petroleum Geologists Bulletin, v. 59, p. 633–664.
- Hentz, T.F., 1994, Sequence stratigraphy of the upper Pennsylvanian Cleveland Formation: A major tight-gas sandstone, western Anadarko Basin, Texas Panhandle: American Association of Petroleum Geologists Bulletin, v. 78, p. 569–595.
- Higley, D.K. and Gaswirth, S.B., 2014, Overview of chapters within USGS DDS-69-EE, chap. 2, *in* Higley, D.K., comp., *Petroleum systems and assessment of undiscovered oil and gas in the Anadarko Basin Province, Colorado, Kansas, Oklahoma, and Texas—USGS Province 58*: U.S. Geological Survey Digital Data Series DDS-69-EE, 5 p.
- Higley, D.K., Gaswirth, S.B., Abbott, M.M., Charpentier, R.R., Cook, T.A., Ellis, G.S., Gianoutsos, N.J., Hatch, J.R., Klett, T.R., Nelson, P., Pawlewicz, M.J., Pearson, O.N., Pollastro, R.M., and Schenk, C.J., 2011, Assessment of undiscovered oil and gas resources of the Anadarko Basin Province of Oklahoma, Kansas, Texas, and Colorado, 2010: U.S. Geological Survey Fact Sheet 2011–3003, 2 p.
- Higley, D.K., Gianoutsos, N.J., Pantea, M.P., and Strickland, S.M., 2014, Precambrian to ground surface grid cell maps of the Anadarko Basin Province, chap. 13, *in* Higley, D.K., compiler, *Petroleum systems and assessment of undiscovered oil and gas in the Anadarko Basin Province, Colorado, Kansas, Oklahoma, and Texas—USGS Province 58*: U.S. Geological Survey Digital Data Series DDS-69-EE, 7 p.
- Huffman, G.G., 1953, Sylvan Shale in northeastern Oklahoma: *Geological Notes*, American Association of Petroleum Geologists Bulletin, v. 37, p. 447–450.
- IHS Energy, 2010, IHS energy production data on CD-ROM: Unpublished database available from IHS Energy, 15 Inverness Way East, Englewood, CO 80112.
- Johnson, K.S., 1989, Geologic evolution of the Anadarko Basin, *in* Johnson, K.S., ed., *Anadarko Basin symposium, 1988*: Oklahoma Geological Survey Circular 90, p. 3–12.
- Johnson, K.S., Amsden, T.W., Denison, R.E., Dutton, S.P., Goldstein, A.G., Rascoe, B., Jr., Sutherland, P.K., and Thompson, D.M., 1988, *in* Sloss, L.L., ed., *Sedimentary cover—North American craton, U.S.: The geology of North America*: Boulder, Colo., Geological Society of America, v. D-2, p. 307–359.
- Keller, G.R., and Baldrige, W.S., 1995, The southern Oklahoma aulacogen, *in* Olsen, K.H., ed., *Continental rifts: Evolution, structure, tectonics*: Amsterdam, Elsevier, p. 427–435.

- Keller, G.R., Lidiak, E.G., Hinze, W.J., and Braile, L.W., 1983, The role of rifting in the tectonic development of the midcontinent, U.S.A.: *Tectonophysics*, v. 94, p. 391–412.
- Keller, G.R., and Stephenson, R.A., 2007, The southern Oklahoma and Dniepr-Donets aulacogens: A comparative analysis, *in* Hatcher, R.D., Jr., Carlson, M.P., McBride, J.H., and Martinez Catalán, J.R., eds., *4-D Framework of continental crust: Geological Society of America Memoir 200*, p. 127–143.
- Kluth, C.F., 1986, Plate tectonics of the Ancestral Rocky Mountains: *American Association of Petroleum Geologists Memoir 41*, p. 353–369.
- Kluth, C.F., and Coney, P.J., 1981, Plate tectonics of the Ancestral Rocky Mountains: *Geology*, v. 9, p. 10–15.
- Kopaska-Merkel, D.C., and Friedman, G.M., 1989, Petrofacies analysis of carbonate rocks: Example from lower Paleozoic Hunton Group of Oklahoma and Texas: *American Association of Petroleum Geologists Bulletin*, v. 73, p. 1289–1306.
- Kuykendall, M.D., and Fritz, R.D., 1993, Misener sandstone: Distribution and relationship to late/post-Hunton unconformities, northern shelf, Anadarko Basin, *in* Johnson, K.S. ed., *Hunton Group core workshop and field trip: Oklahoma Geological Survey Special Publication 93–4*, p. 117–134.
- Luza, K.V., 1989, Neotectonics and seismicity of the Anadarko Basin, *in* Johnson, K.S., ed., *Anadarko Basin symposium, 1988: Oklahoma Geological Survey Circular 90*, p. 121–132.
- Luza, K.V., Madole, R.F., and Crone, A.J., 1987, Investigation of the Meers Fault, southwestern Oklahoma: *Oklahoma Geological Survey Special Publication 87–1*, 75 p.
- Mannhard, G.W., and Busch, D.A., 1974, Stratigraphic trap accumulations in southwestern Kansas and northwestern Oklahoma: *American Association of Petroleum Geologists Bulletin*, v. 58, p. 447–463.
- McConnell, D.A., 1989, Constraints on magnitude and sense of slip across the northern margin of the Wichita uplift, southwestern Oklahoma, *in* Johnson, K.S., ed., *Anadarko Basin symposium, 1988: Oklahoma Geological Survey Circular 90*, p. 85–96.
- Perry, W.J., Jr., 1989, Tectonic evolution of the Anadarko Basin region, Oklahoma: *U.S. Geological Survey Bulletin 1866-A*, p. A1–A19.
- Rascoe, B., Jr., 1962, Regional stratigraphic analysis of Pennsylvanian and Permian rocks in western mid-continent, Colorado, Kansas, Oklahoma, Texas: *American Association of Petroleum Geologists Bulletin*, v. 46, p. 1345–1370.
- Rascoe, B., Jr., and Adler, F.J., 1983, Permo-Carboniferous hydrocarbon accumulations, mid-continent, U.S.A.: *American Association of Petroleum Geologists Bulletin*, v. 67, p. 979–1001.
- Schramm, M.W., 1964, Paleogeologic and quantitative lithofacies analysis, Simpson Group, Oklahoma: *Bulletin of the American Association of Petroleum Geologists*, v. 48, p. 1164–1195.
- Shatsky, N.S., 1946, The great Donets Basin and the Wichita system: Comparative tectonics of ancient platforms: *Akademiya Nauk SSSR Izvestiya, Seriya Geologicheskaya*, v. 6, p. 57–90.
- Thomas, W.A., 1989, The Appalachian-Ouachita orogen beneath the Gulf Coastal Plain between the outcrops in the Appalachian and Ouachita Mountains, *in* Hatcher, R.D., Jr., Thomas, W.A., and Viele, G.W., eds., *The Appalachian-Ouachita orogen in the United States: Geological Society of America, The Geology of North America*, v. F–2, p. 537–553.
- Thomas, W.A., 1991, The Appalachian-Ouachita rifted margin of southeastern North America: *Geological Society of America Bulletin*, v. 103, p. 415–431.
- Thomas, W.A., 2006, Tectonic inheritance at a continental margin: *GSA Today*, v. 16, p. 4–11.
- Thomas, W.A., and Astini, R.A., 1996, The Argentine Precordillera: A traveler from the Ouachita embayment of North American Laurentia: *Science*, v. 273, p. 752–757.
- Tomlinson, C.W., and McBee, W., Jr., 1959, Pennsylvanian sediments and orogenies of Ardmore District, Oklahoma, *in* *Petroleum geology of southern Oklahoma, volume 2: American Association of Petroleum Geologists*, p. 3–52.
- Van Schmus, W.R., Bickford, M.E., and Turek, E., 1996, Proterozoic geology of the east-central mid-continent basement, *in* van der Pluijm, B.A., and Catacosinos, P.A., eds., *Basement and basins of eastern North America: Geological Society of America Special Paper 308*, p. 7–32.
- Van Schmus, W.R., Schneider, D.A., Holm, D.K., Dodson, S., and Nelson, B.K., 2007, New insights into the southern margin of the Archean-Proterozoic boundary in the north-central United States based on U-Pb, Sm-Nd, and Ar-Ar geochronology: *Precambrian Research*, v. 157, p. 80–105.
- Whitmeyer, S.J., and Karlstrom, K.E., 2007, Tectonic model for the Proterozoic growth of North America: *Geosphere*, v. 3, p. 220–259.
- Wilson, J.T., 1966, Did the Atlantic close and then reopen?: *Nature*, v. 211, p. 676–681.